Geophys. J. Int. (2009) **178,** 1289–1304 doi: 10.1111/j.1365-246X.2009.04201.x

Interferometric seismoelectric Green's function representations

Sjoerd A. L. de Ridder,* Evert Slob and Kees Wapenaar

Department of Geotechnology, Delft University of Technology, 2600 *GA Delft, the Netherlands. E-mail: ridder@stanford.edu*

Accepted 2009 April 3. Received 2009 March 27; in original form 2008 July 28

SUMMARY

Interferometric Green's function representations can be used to retrieve a Green's function between two receiver stations, effectively turning one receiver into a source. Through reciprocity theorems of the convolution and correlation types, we derive interferometric Green's function representations for coupled electromagnetic and seismic wave propagation in 1-D. These representations express a symmetrized Green's function in terms of correlations of sources distributed throughout the domain of reciprocity and on its boundary. The main challenge for practical implementation is the necessity of sources throughout a domain. Numerical examples show how this constraint can be relaxed for different configurations. In a configuration of two layers bounded by a vacuum, seismic noise sources behind the interface can be used to recover seismoelectric reflection responses that suffer from small amplitude losses, but are not corrupted by spurious events.

Key words: Interferometry; Electromagnetic theory; Theoretical seismology; Wave propagation.

1 INTRODUCTION

Seismic interferometry for passive seismics is a novel geophysical tool to generate Green's functions by cross-correlation of recorded background noise. Based on randomness of the wavefield in a 2-D homogeneous plane, Aki (1957) showed how a frequency domain 2-D wavefunction can be retrieved by evaluating a spatial autocorrelation coefficient. The principle for deterministic wavefields in inhomogeneous media was first derived by Claerbout (1968), who showed that the reflection response of an acoustic 1-D horizontally layered medium bounded by a free-surface can be synthesized from the autocorrelation of its transmission response. Weaver & Lobkis (2001) showed how the 3-D Green's function of a virtual pulse echo experiment emerges from the cross-correlation of recordings of a diffuse wavefield. Similar results, based upon the diffusivity of the recorded wavefield, were shown by various authors to hold for open and closed configurations (Lobkis & Weaver 2001; van Tiggelen 2003; Malcolm *et al.* 2004; Snieder 2004; Roux *et al.* 2005; Shapiro *et al.* 2005).

Claerbouts principle for deterministic wavefields in 1-D media was extended to hold for arbitrarily inhomogeneous media in 3-D (Wapenaar *et al.* 2002; Derode *et al.* 2003; Wapenaar 2004). So far, Green's function retrieval by cross-correlation was thought to hold only for lossless media, until Roux *et al.* (2005) treated a homogeneous lossy space theoretically. A more general analysis was performed by Slob *et al.* (2006) who showed the effects of conductivity in electromagnetic Green's function retrieval and Snieder (2006) who showed how a volume distribution of sources can be used to retrieve Green's functions of a diffusion system. A general derivation for any deterministic linear flow, diffusion or wave phenomena in 3-D inhomogeneous media based upon reciprocity theorems is presented by Wapenaar *et al.* (2006).

The application of interferometric Green's function retrieval techniques to seismoelectric phenomena could potentially address challenging problems in seismoelectric surveys. Sources in seismoelectric surveys need to be strong but receivers could be positioned where such strong sources are not desirable. In addition, the inherent ability of interferometry to cumulatively stack the recorded background noise might help overcome the weak signal to noise ratio in conventional seismoelectric surveys.

Pride (1994) derived a system of equations for coupled electromagnetic and seismic waves in saturated porous media. Pride & Haartsen (1996) derived the reciprocity theorem of the convolution type and a power balance in its local form for seismoelectric waves. Wapenaar (2003) extended this result to a correlation-type reciprocity theorem for seismoelectric waves. Here we use seismoelectric reciprocity theorems to derive an interferometric integral representation for seismoelectric Green's functions in 1-D. This representation consists of two terms, one

*Now at: Department of Geophysics, Stanford University, CA 94305-2215, USA.

representing correlations of recorded responses of sources throughout the domain of reciprocity and one representing correlations of recorded responses of sources on the boundary of the domain of reciprocity.

Three examples are analysed to explore the potential use of the interferometric seismoelectric Green's function representation in practise. The first configuration is a homogeneous medium, which is extended to a medium consisting of two half-spaces in the second example, and the third configuration is a two-layer medium bounded by vacuum. These examples show the contributions to the retrieved result of the domain and boundary integrals, as well as the contributions of several source positions in the domain integral.

2 SEISMOELECTRIC SYSTEM OF EQUATIONS IN 1-D

We use the system of equations for coupling between electromagnetic and seismic waves in saturated porous media as derived by Pride (1994). Pride's system comprises four wave types, one electromagnetic wave, one elastodynamic shear wave and two pressure waves. In a 1-D setting the electromagnetic and elastodynamic shear waves decouple from the pressure waves, see Appendix A. Then all fields are scalar quantities. We have the electric field strength $E = E(x, t)$ in (V m^{-1}),the magnetic field strength $H = H(x,t)$ in (A m^{-1}), the elastic particle velocity of the solid phase $v^s = v^s(x, t)$ in (m s^{-1}) and the shear stress in the bulk $\tau^b = \tau^b(x, t)$ in (N m^{-2}). The coupling coefficient $\mathcal{L} = \mathcal{L}(x, t)$ in (m^{2}s V^{-1}) is a time-convolution operator (Pride 1994). Here we consider the electric and magnetic constitutive parameters $\epsilon^{f,s} = \epsilon^{f,s}(x)$ in [s(Ω m)$^{-1}$] and $\sigma = \sigma(x)$ in [(Ω m)$^{-1}$], and $\mu = \mu_0$ in (Ω s m^{-1}) as time-independent. They are respectively, the electric permittivity in the fluid and solid phases and electric conductivity, while for the magnetic permeability we take its value in vacuum. The seismic constitutive parameters are the density of the fluid and solid phases $\rho^{f,s} = \rho^{f,s}(x)$ in (kg m^{-3}) and the shear modulus of the framework of grains $N = N(x)$ in (N m^{-2}). Finally, we have the fluid viscosity $\eta = \eta(x)$ in (Ns m^{-2}) and the hydraulic permeability $k = k(x)$ in (m^2). Then there are four possible source terms, the electric and magnetic current source densities $J^e = J^e(x, t)$ in (A m^{-2}) and $J^m = J^m(x, t)$ in (V m^{-2}). The modified force source $f = f(x, t)$ in (N m^{-3}) and the external deformation rate $h^b = h^b(x, t)$ in (s^{-1}). We derive the representations in the frequency domain and define the temporal Fourier transform of a time dependent function $f(t)$ as

$$\mathcal{F}\{f(t)\} = \hat{f}(\omega) = \int_{-\infty}^{\infty} f(t)\mathrm{e}^{-\mathrm{i}\omega t}\,\mathrm{d}t. \tag{1}$$

The four equations governing the 1-D seismoelectric system in the frequency domain are

$$\mathrm{i}\omega\hat{\varepsilon}\hat{E} - \mathrm{i}\omega\rho^f\hat{\mathcal{L}}\hat{v}^s - \partial_x\hat{H} = -\hat{J}^e, \tag{2}$$

$$\mathrm{i}\omega\mu\hat{H} - \partial_x\hat{E} = -\hat{J}^m, \tag{3}$$

$$\mathrm{i}\omega\hat{\rho}^c\hat{v}^s + \mathrm{i}\omega\rho^f\hat{\mathcal{L}}\hat{E} - \partial_x\hat{\tau}^b = \hat{f}, \tag{4}$$

$$-\mathrm{i}\omega N^{-1}\hat{\tau}^b + \partial_x\hat{v}^s = \hat{h}^b, \tag{5}$$

where ∂_x denotes a spatial derivative. These are Maxwell's equations, (2) and (3), with a coupling term to the particle velocity. Eq. (4) is the equation of motion for the particle velocity in the solid and the shear stress in the bulk with a coupling term to the electric field strength and eq. (5) is the stress–strain relation. In eq. (2), the complex effective electric permittivity is introduced as $\hat{\varepsilon} = \hat{\varepsilon}(x, \omega)$ and it is given by $\hat{\varepsilon} = \frac{\phi}{\alpha_\infty}(\epsilon^f - \epsilon^s) + \epsilon^s - \mathrm{i}\sigma/\omega$, where ϕ denotes porosity and α_∞ denotes tortuosity. In eq. (4), the complex effective bulk density is introduced as $\hat{\rho}^c = \hat{\rho}^c(x, \omega)$ and it is given by $\hat{\rho}^c = [\rho^b - \mathrm{i}\omega(\rho^f)^2 k/\eta]$, where the bulk density is obtained from effective medium theory as $\rho^b = (1 - \phi)\rho^s + \phi\rho^f$ assuming a fully saturated medium. Following Wapenaar & Fokkema (2004) this system can be ordered into a matrix equation of the form

$$\mathrm{i}\omega\hat{\mathbf{A}}\hat{\mathbf{u}} + \mathbf{D}_x\hat{\mathbf{u}} = \hat{\mathbf{s}}, \tag{6}$$

such that the field vector $\hat{\mathbf{u}}$ and the source vector $\hat{\mathbf{s}}$ are given by

$$\hat{\mathbf{u}} = (\hat{E}, \hat{H}, \hat{v}^s, -\hat{\tau}^b)^T, \quad \hat{\mathbf{s}} = (-\hat{J}^e, -\hat{J}^m, \hat{f}, \hat{h}^b)^T, \tag{7}$$

where T denotes matrix transposition. The matrix $\hat{\mathbf{A}}$ contains medium parameters and the matrix $\mathbf{D}_x$ contains spatial derivatives,

$$\hat{\mathbf{A}} = \begin{pmatrix} \hat{\varepsilon} & 0 & -\rho^f\hat{\mathcal{L}} & 0 \\ 0 & \mu & 0 & 0 \\ \rho^f\hat{\mathcal{L}} & 0 & \hat{\rho}^c & 0 \\ 0 & 0 & 0 & N^{-1} \end{pmatrix}, \qquad \mathbf{D}_x = \begin{pmatrix} 0 & -\partial_x & 0 & 0 \\ -\partial_x & 0 & 0 & 0 \\ 0 & 0 & 0 & \partial_x \\ 0 & 0 & \partial_x & 0 \end{pmatrix}. \tag{8}$$

Note how the matrices $\mathbf{A}$ and $\mathbf{D}_x$ obey symmetry properties

$$\hat{\mathbf{A}} = \mathbf{K}\hat{\mathbf{A}}^T\mathbf{K} \quad \text{and} \quad \mathbf{D}_x = -\mathbf{K}\mathbf{D}_x^T\mathbf{K}, \tag{9}$$

where the diagonal matrix $\mathbf{K}$ is given as

$$\mathbf{K} = \mathrm{diag}\,(-1, 1, 1, -1)\,. \tag{10}$$

We introduce the Fourier domain Green's functions of this system by replacing one element of the source vector $\hat{\mathbf{s}}$ by the Fourier domain of an impulsive source acting at $t = 0$ s and at $x = x_s$. $\hat{\mathbf{s}} \rightarrow \mathbf{I}\delta(x - x_s)$, we correspondingly replace the field vector by a Green's matrix

$\hat{\mathbf{u}} \rightarrow \hat{\mathbf{G}}(x, x_{\rm s}, \omega)$. The Green's matrix obeys the matrix eq. (6),

$$\mathrm{i}\omega\hat{\mathbf{A}}\hat{\mathbf{G}}(x, x_{\rm s}, \omega) + \mathbf{D}_{\rm x}\hat{\mathbf{G}}(x, x_{\rm s}, \omega) = \mathbf{I}\delta(x - x_{\rm s}). \tag{11}$$

All elements of the Green's matrix have dimension (m^{-1}) and are distinguished by their superscript containing the field type and source type, the Green's matrix for the 1-D seismoelectric system is given by

$$\hat{\mathbf{G}}(x, x_{\rm s}, \omega) = \begin{bmatrix} \hat{G}^{E,J^e}(x, x_{\rm s}, \omega) & \hat{G}^{E,J^m}(x, x_{\rm s}, \omega) & \hat{G}^{E,f}(x, x_{\rm s}, \omega) & \hat{G}^{E,h^b}(x, x_{\rm s}, \omega) \\ \hat{G}^{H,J^e}(x, x_{\rm s}, \omega) & \hat{G}^{H,J^m}(x, x_{\rm s}, \omega) & \hat{G}^{H,f}(x, x_{\rm s}, \omega) & \hat{G}^{H,h^b}(x, x_{\rm s}, \omega) \\ \hat{G}^{v^s,J^e}(x, x_{\rm s}, \omega) & \hat{G}^{v^s,J^m}(x, x_{\rm s}, \omega) & \hat{G}^{v^s,f}(x, x_{\rm s}, \omega) & \hat{G}^{v^s,h^b}(x, x_{\rm s}, \omega) \\ \hat{G}^{\tau^b,J^e}(x, x_{\rm s}, \omega) & \hat{G}^{\tau^b,J^m}(x, x_{\rm s}, \omega) & \hat{G}^{\tau^b,f}(x, x_{\rm s}, \omega). & \hat{G}^{\tau^b,h^b}(x, x_{\rm s}, \omega) \end{bmatrix}. \tag{12}$$

The notation $\hat{G}^{v^s,J^e}(x, x_{\rm s}, \omega)$ denotes a particle velocity response measured at x due to an impulsive electrical current source acting at $x = x_{\rm s}$, in the frequency domain. In Appendix B, we derive Green's function solutions for a homogeneous medium. The scalar part of the Green's matrix can be seen to contain two events travelling with different velocities,

$$\hat{G}^s(x, x_{\rm s}, \omega) = \frac{\hat{G}^s_{\rm te}(x, x_{\rm s}, \omega) - \hat{G}^s_{\rm sh}(x, x_{\rm s}, \omega)}{\{\mathrm{i}\omega\hat{s}_{\rm sh}\}^2 - \{\mathrm{i}\omega\hat{s}_{\rm te}\}^2}, \tag{13}$$

where $\hat{s}_{\rm sh}$ and $\hat{s}_{\rm te}$ are the seismic and electromagnetic slownesses, respectively. Because $\hat{s}_{\rm sh} \gg \hat{s}_{\rm te}$, the seismic slowness dominates the scaling of the scalar part of the seismoelectric Green's function in homogeneous media. The partial Green's functions $\hat{G}^s_{\rm sh}(x, x_{\rm s}, \omega)$ and $\hat{G}^s_{\rm te}(x, x_{\rm s}, \omega)$ are each, respectively, given by

$$\hat{G}^s_{\rm sh;te}(x, x_{\rm s}, \omega) = \frac{\exp\left(-\mathrm{i}\omega\hat{s}_{\rm sh;te}\,|x - x_{\rm s}|\right)}{2\mathrm{i}\omega\hat{s}_{\rm sh;te}}. \tag{14}$$

This means that seismoelectric conversion takes place at the source and at the receiver. This can be understood from eqs (2) to (5). An electrical current source excites both the electric and magnetic fields as well as the particle velocity through the coupling coefficient. In heterogeneous media conversion of wave types will also occur at interfaces where the material properties change (Haartsen & Pride 1997).

3 CONVOLUTION TYPE RECIPROCITY THEOREM

A reciprocity theorem interrelates two independent states in one and the same domain (de Hoop 1966; Fokkema & van den Berg 1993). The basis for reciprocity theorems is the application of the theorem of Gauss over an interaction quantity that interrelates the two states. We consider two physical states, distinguished with subscripts A and B, in a 1-D domain $\mathbb{D}$, with boundary points $x = x_1$ and $x = x_2$ and outward pointing normals n_1 and n_2. We choose $x_1 < x_2$ and find outward pointing normal vectors $n_1 = -1$ and $n_2 = 1$. The material parameters and the source functions may be different in both states. We consider the interaction quantity

$$\partial_x\left(\hat{E}_A\hat{H}_B - \hat{H}_A\hat{E}_B + \hat{\tau}^b_A\hat{v}^s_B - \hat{v}^s_A\hat{\tau}^b_B\right). \tag{15}$$

This interaction quantity is the summation of the convolution type interaction quantities commonly used in the uncoupled electromagnetic and elastodynamic systems (de Hoop 1995; Wapenaar 2003). Substitution of eqs (2)–(5) for the fields in states A and B into eq. (15), integrating over the domain $\mathbb{D}$ from x_1 to x_2 and applying the theorem of Gauss, leads to the convolution type reciprocity theorem

$$\begin{aligned} &\left\{\hat{E}_A\hat{H}_B - \hat{H}_A\hat{E}_B + \hat{\tau}^b_A\hat{v}^s_B - \hat{v}^s_A\hat{\tau}^b_B\right\}\Big|_{x_1}^{x_2} \\ &\quad= \int_{\mathbb{D}}\left\{\hat{E}_A\hat{J}^e_B - \hat{E}_B\hat{J}^e_A + \hat{H}_A\hat{J}^m_B - \hat{H}_B\hat{J}^m_A + \hat{v}^s_A\hat{f}_B - \hat{v}^s_B\hat{f}_A + \hat{\tau}^b_A\hat{h}^b_B - \hat{\tau}^b_B\hat{h}^b_A\right\}\mathrm{d}x \\ &\qquad+ \mathrm{i}\omega\int_{\mathbb{D}}\left\{-\hat{E}_A\left(\hat{\varepsilon}_A - \hat{\varepsilon}_B\right)\hat{E}_B + \hat{E}_A\left(\rho^f_A\hat{\mathcal{L}}_A - \rho^f_B\hat{\mathcal{L}}_B\right)\hat{v}^s_B + \hat{v}^s_A\left(\rho^f_A\hat{\mathcal{L}}_A - \rho^f_B\hat{\mathcal{L}}_B\right)\hat{E}_B\right. \\ &\qquad\left.+ \hat{v}^s_A\left(\hat{\rho}^c_A - \hat{\rho}^c_B\right)\hat{v}^s_B + \hat{H}_A\left(\mu_A - \mu_B\right)\hat{H}_B - \hat{\tau}^b_A\left(N^{-1}_A - N^{-1}_B\right)\hat{\tau}^b_B\right\}\mathrm{d}x. \end{aligned} \tag{16}$$

This is the 1-D equivalent of the convolution type reciprocity integral for the full 3-D seismoelectric system of Pride, previously derived by Wapenaar (2003). We speak of a convolution type reciprocity theorem, because the multiplications in the frequency domain correspond to convolutions in the time domain. A similar equation for the general matrix eq. (6) was derived by Wapenaar & Fokkema (2004),

$$\left\{\hat{\mathbf{u}}^T_A\mathbf{K}\mathbf{N}_{\rm x}\hat{\mathbf{u}}_B\right\}\Big|_{x_1}^{x_2} = \int_{\mathbb{D}}\left\{\hat{\mathbf{u}}^T_A\mathbf{K}\hat{\mathbf{s}}_B - \hat{\mathbf{s}}^T_A\mathbf{K}\hat{\mathbf{u}}_B\right\}\mathrm{d}x + \mathrm{i}\omega\int_{\mathbb{D}}\left\{\hat{\mathbf{u}}^T_A\mathbf{K}\left[\hat{\mathbf{A}}_A - \hat{\mathbf{A}}_B\right]\hat{\mathbf{u}}_B\right\}\mathrm{d}x, \tag{17}$$

where $\mathbf{N}_{\rm x}$ is a matrix containing normal vectors arising after the application of the theorem of Gauss, it has the same structure as the matrix $\mathbf{D}_{\rm x}$ but with all partial derivatives replaced by the unit value,

$$\mathbf{N}_{\rm x} = \begin{pmatrix} 0 & -1 & 0 & 0 \\ -1 & 0 & 0 & 0 \\ 0 & 0 & 0 & 1 \\ 0 & 0 & 1 & 0 \end{pmatrix}. \tag{18}$$

We choose impulsive sources in state A at $x = x_A$ and in state B at $x = x_B$ both inside an arbitrarily inhomogeneous domain $\mathbb{D}$ with perfect interfaces, such that $x_1 \leq x_A, x_B \leq x_2$. After substitution of the Green's matrices $\hat{\mathbf{G}}(x, x_A, \omega)$ and $\hat{\mathbf{G}}(x, x_B, \omega)$ into eq. (17), we find

$$\begin{aligned}&\hat{\mathbf{G}}^T(x_\mathrm{B}, x_\mathrm{A}, \omega)\mathbf{K} - \mathbf{K}\hat{\mathbf{G}}(x_A, x_B, \omega)\\ &\quad = \left\{\hat{\mathbf{G}}^T(x, x_A, \omega)\mathbf{K}\mathbf{N}_\mathrm{x}\hat{\mathbf{G}}(x, x_B, \omega)\right\}\Big|_{x_1}^{x_2} - \int_{\mathbb{D}} \left\{\hat{\mathbf{G}}^T(x, x_A, \omega)\mathbf{K}[\mathrm{i}\omega(\hat{\mathbf{A}}_A - \hat{\mathbf{A}}_B)]\hat{\mathbf{G}}(x, x_B, \omega)\right\} \mathrm{d}x.\end{aligned} \tag{19}$$

If we choose equal medium parameters in states A and B, and choose the boundary $\partial\mathbb{D}$ at infinity, the right-hand side of eq. (19) vanishes and we find the reciprocity relation for the Green's matrix (Wapenaar *et al.* 2006),

$$\hat{\mathbf{G}}(x_A, x_B, \omega) = \mathbf{K}\hat{\mathbf{G}}^T(x_B, x_A, \omega)\mathbf{K}, \tag{20}$$

where we used $\mathbf{K} = \mathbf{K}^{-1}$. When we expand eq. (20) using the Green's matrix in eq. (12) and the matrix $\mathbf{K}$ in eq. (10), we find the following source–receiver reciprocity relations,

$$\hat{G}^{E,J^e}(x_\mathrm{A}, x_\mathrm{B}, \omega) = \hat{G}^{E,J^e}(x_\mathrm{B}, x_\mathrm{A}, \omega), \qquad \hat{G}^{H,J^e}(x_\mathrm{A}, x_\mathrm{B}, \omega) = -\hat{G}^{E,J^m}(x_\mathrm{B}, x_\mathrm{A}, \omega), \tag{21}$$

$$\hat{G}^{v^s,J^e}(x_\mathrm{A}, x_\mathrm{B}, \omega) = -\hat{G}^{E,f}(x_\mathrm{B}, x_\mathrm{A}, \omega), \qquad \hat{G}^{\tau^b,J^e}(x_\mathrm{A}, x_\mathrm{B}, \omega) = \hat{G}^{E,h^b}(x_\mathrm{B}, x_\mathrm{A}, \omega), \tag{22}$$

$$\hat{G}^{H,J^m}(x_\mathrm{A}, x_\mathrm{B}, \omega) = \hat{G}^{H,J^m}(x_\mathrm{B}, x_\mathrm{A}, \omega), \qquad \hat{G}^{v^s,f}(x_\mathrm{A}, x_\mathrm{B}, \omega) = \hat{G}^{v^s,f}(x_\mathrm{B}, x_\mathrm{A}, \omega), \tag{23}$$

$$\hat{G}^{\tau^b,h^b}(x_\mathrm{A}, x_\mathrm{B}, \omega) = \hat{G}^{\tau^b,h^b}(x_\mathrm{B}, x_\mathrm{A}, \omega), \qquad \hat{G}^{v^s,J^m}(x_\mathrm{A}, x_\mathrm{B}, \omega) = \hat{G}^{H,f}(x_\mathrm{B}, x_\mathrm{A}, \omega), \tag{24}$$

$$\hat{G}^{\tau^b,J^m}(x_\mathrm{A}, x_\mathrm{B}, \omega) = -\hat{G}^{H,h^b}(x_\mathrm{B}, x_\mathrm{A}, \omega), \qquad \hat{G}^{\tau^b,f}(x_\mathrm{A}, x_\mathrm{B}, \omega) = -\hat{G}^{v^s,h^b}(x_\mathrm{B}, x_\mathrm{A}, \omega). \tag{25}$$

4 CORRELATION TYPE RECIPROCITY THEOREM

Instead of choosing both states in forward time, we combine the two states with state A in time-reversed state. This amounts to complex conjugation in the frequency domain, denoted by an asterisk in superscript *. The field equations in state A now satisfy

$$-\mathrm{i}\omega\hat{\varepsilon}^*\hat{E}^* + \mathrm{i}\omega\rho^f\hat{\mathcal{L}}\hat{v}^{s*} - \partial_x\hat{H}^* = -\hat{J}^{e*}, \tag{26}$$

$$-\mathrm{i}\omega\mu\hat{H}^* - \partial_x\hat{E}^* = -\hat{J}^{m*}, \tag{27}$$

$$-\mathrm{i}\omega\hat{\rho}^{c*}\hat{v}^{s*} - \mathrm{i}\omega\rho^f\hat{\mathcal{L}}\hat{E}^* - \partial_x\hat{\tau}^{b*} = \hat{f}^*, \tag{28}$$

$$\mathrm{i}\omega N^{-1}\hat{\tau}^{b*} + \partial_x\hat{v}^{s*} = \hat{h}^{b*}. \tag{29}$$

The time dependent medium properties $\hat{\varepsilon}^*$, $\hat{\rho}^{c*}$ now represent time-reversed causal functions, thus the media become dissipative in progressive negative time. We start from the interaction quantity,

$$-\partial_x\left(\hat{E}_A^*\hat{H}_B + \hat{H}_A^*\hat{E}_B + \hat{\tau}_A^{b*}\hat{v}_B^s + \hat{v}_A^{s*}\hat{\tau}_B^b\right). \tag{30}$$

Substitution of eqs (2)–(5) for the fields in state B and eqs (26)–(29) for the fields in state A, into eq. (30), integrating over the domain $\mathbb{D}$ from x_1 to x_2 and applying the theorem of Gauss, leads to the correlation type reciprocity theorem

$$\begin{aligned}&-\left\{\hat{E}_\mathrm{A}^*\hat{H}_\mathrm{B} + \hat{H}_\mathrm{A}^*\hat{E}_\mathrm{B} + \hat{\tau}_\mathrm{A}^{b*}\hat{v}_\mathrm{B}^s + \hat{v}_\mathrm{A}^{s*}\hat{\tau}_\mathrm{B}^b\right\}\Big|_{x_1}^{x_2}\\ &\quad = \int_{\mathbb{D}}\left\{-\hat{E}_\mathrm{B}\hat{J}_\mathrm{A}^{e*} - \hat{E}_\mathrm{A}^*\hat{J}_\mathrm{B}^e - \hat{H}_\mathrm{B}\hat{J}_\mathrm{A}^{m*} - \hat{H}_\mathrm{A}^*\hat{J}_\mathrm{B}^m + \hat{v}_\mathrm{A}^{s*}\hat{f}_\mathrm{B} + \hat{v}_\mathrm{B}^s\hat{f}_\mathrm{A}^* - \hat{\tau}_\mathrm{B}^b\hat{h}_\mathrm{A}^{b*} - \hat{\tau}_\mathrm{A}^{b*}\hat{h}_\mathrm{B}^b\right\}\mathrm{d}x\\ &\qquad - \mathrm{i}\omega\int_{\mathbb{D}}\left\{\hat{E}_\mathrm{A}^*\left(\hat{\varepsilon}_B - \hat{\varepsilon}_A^*\right)\hat{E}_\mathrm{B} - \hat{E}_\mathrm{A}^*\left(\rho_B^f\hat{\mathcal{L}}_B + \rho_A^f\hat{\mathcal{L}}_A\right)\hat{v}_\mathrm{B}^s + \hat{v}_\mathrm{A}^*\left(\rho_B^f\hat{\mathcal{L}}_B + \rho_A^f\hat{\mathcal{L}}_A\right)\hat{E}_\mathrm{B}\right.\\ &\qquad \left. + \hat{H}_\mathrm{A}^*\left(\mu_B - \mu_A\right)\hat{H}_\mathrm{B} + \hat{v}_\mathrm{A}^{s*}\left(\hat{\rho}_B^c - \hat{\rho}_A^{c*}\right)\hat{v}_\mathrm{B}^s + \hat{\tau}_\mathrm{A}^{b*}\left(N_B^{-1} - N_A^{-1}\right)\hat{\tau}_\mathrm{B}^b\right\}\mathrm{d}x,\end{aligned} \tag{31}$$

which is the 1-D equivalent of the correlation type reciprocity integral for the full 3-D seismoelectric system of Pride previously derived by Wapenaar (2003). We speak of a correlation type reciprocity theorem, because the multiplications with the complex conjugate fields in the frequency domain correspond to correlations in the time domain. A similar equation for the general matrix eq. (6) was derived by Wapenaar & Fokkema (2004),

$$\left\{\hat{\mathbf{u}}_A^\dagger\mathbf{N}_\mathrm{x}\hat{\mathbf{u}}_B\right\}\Big|_{x_1}^{x_2} = \int_{\mathbb{D}}\left\{\hat{\mathbf{u}}_A^\dagger\hat{\mathbf{s}}_B + \hat{\mathbf{s}}_A^\dagger\hat{\mathbf{u}}_B\right\}\mathrm{d}x + \mathrm{i}\omega\int_{\mathbb{D}}\left\{\hat{\mathbf{u}}_A^\dagger\left[\hat{\mathbf{A}}_A^\dagger - \hat{\mathbf{A}}_B\right]\hat{\mathbf{u}}_B\right\}\mathrm{d}x, \tag{32}$$

where $\dagger$ denotes matrix transposition and complex conjugation. We choose impulsive sources in state A at $x = x_A$ and in state B at $x = x_B$ both inside an arbitrarily heterogeneous domain $\mathbb{D}$ with perfect interfaces, such that $x_1 \leq x_A, x_B \leq x_2$. After substitution of the Green's matrices

$\hat{\mathbf{G}}(x, x_A, \omega)$ and $\hat{\mathbf{G}}(x, x_B, \omega)$ into eq. (32), and using the symmetry property of the Green's matrix of eq. (20) we find

$$\begin{aligned}&\hat{\mathbf{G}}(x_A, x_B, \omega) + \hat{\mathbf{G}}^{\dagger}(x_B, x_A, \omega)\\ &\quad= \left\{\hat{\mathbf{G}}^{\dagger}(x, x_A, \omega)\mathbf{N}_{\mathrm{x}}\hat{\mathbf{G}}(x, x_B, \omega)\right\}\Big|_{x_1}^{x_2} + \int_{\mathbb{D}}\left\{\hat{\mathbf{G}}^{\dagger}(x, x_A, \omega)\left[\mathrm{i}\omega\left(\hat{\mathbf{A}}_B - \hat{\mathbf{A}}_A^{\dagger}\right)\right]\hat{\mathbf{G}}(x, x_B, \omega)\right\}\mathrm{d}x.\end{aligned} \tag{33}$$

4.1 Interferometric Green's function representation

A third integral representation is a novel interpretation of the correlation type reciprocity theorem. Applying the source receiver reciprocity relation for the Green's matrix into the correlation type reciprocity theorem for the Green's matrix, eq. (33), using the symmetry properties of the matrices $\mathbf{D}_{\mathrm{x}}$ and $\hat{\mathbf{A}}$ and transposing the entire equation, we find

$$\begin{aligned}&\hat{\mathbf{G}}(x_B, x_A, \omega) + \hat{\mathbf{G}}^{\dagger}(x_A, x_B, \omega)\\ &\quad= \left\{\hat{\mathbf{G}}(x_B, x, \omega)\mathbf{N}_{\mathrm{x}}\hat{\mathbf{G}}^{\dagger}(x_A, x, \omega)\right\}\Big|_{x_1}^{x_2} + \int_{\mathbb{D}}\left\{\hat{\mathbf{G}}(x_B, x, \omega)\left[\mathrm{i}\omega\left(\hat{\mathbf{A}}_B - \hat{\mathbf{A}}_A^{\dagger}\right)\right]\hat{\mathbf{G}}^{\dagger}(x_A, x, \omega)\right\}\mathrm{d}x,\end{aligned} \tag{34}$$

which is the interferometric Green's function representation as derived by Wapenaar *et al.* (2006). We expand the $\{1, 3\}$ element of the left-hand side of eq. (34), using the Green's matrix of eq. (12) and the normal vectors in $\mathbf{N}_{\mathrm{x}}$ of eq. (18), assuming that states A and B have equal medium parameters, and the sources emit a signal with a power spectrum $\hat{S}$,

$$\begin{aligned}&\left\{\hat{G}^{E,f}(x_{\mathrm{B}}, x_{\mathrm{A}}, \omega) + \hat{G}^{v^s,J^e*}(x_{\mathrm{A}}, x_{\mathrm{B}}, \omega)\right\}\hat{S}\\ &\quad= \Big\{\hat{G}^{E,J^e}(x_{\mathrm{B}}, x, \omega)\hat{G}^{v,J^m*}(x_{\mathrm{A}}, x, \omega) + \hat{G}^{E,J^m}(x_{\mathrm{B}}, x, \omega)\hat{G}^{v,J^e*}(x_{\mathrm{A}}, x, \omega)\\ &\qquad- \hat{G}^{E,f}(x_{\mathrm{B}}, x, \omega)\hat{G}^{v,h*}(x_{\mathrm{A}}, x, \omega) - \hat{G}^{E,h}(x_{\mathrm{B}}, x, \omega)\hat{G}^{v,f*}(x_{\mathrm{A}}, x, \omega)\Big\}\Big|_{x_1}^{x_2}\ \hat{S}\\ &\qquad+ \mathrm{i}\omega 2\int_{\mathbb{D}}\Big\{\hat{G}^{E,J^e}(x_{\mathrm{B}}, x, \omega)\mathrm{i}\Im\{\hat{\varepsilon}\}\hat{G}^{v,J^e*}(x_{\mathrm{A}}, x, \omega) + \hat{G}^{E,f}(x_{\mathrm{B}}, x, \omega)\Re\{\rho^f\hat{\mathcal{L}}\}\hat{G}^{v,J^e*}(x_{\mathrm{A}}, x, \omega)\\ &\qquad- \hat{G}^{E,J^e}(x_{\mathrm{B}}, x, \omega)\Re\{\rho^f\hat{\mathcal{L}}\}\hat{G}^{v,f*}(x_{\mathrm{A}}, x, \omega) + \hat{G}^{E,f}(x_{\mathrm{B}}, x, \omega)i\Im\{\hat{\rho}^c\}\hat{G}^{v,f*}(x_{\mathrm{A}}, x, \omega)\Big\}\mathrm{d}x\ \hat{S}.\end{aligned} \tag{35}$$

According to source–receiver reciprocity expressed in eq. (22), we have $\hat{G}^{v^s,J^e}(x_{\mathrm{A}}, x_{\mathrm{B}}, \omega) = -\hat{G}^{E,f}(x_{\mathrm{B}}, x_{\mathrm{A}}, \omega)$. Thus on the left-hand side side of eq. (35) we retrieve $i\,2\,\Im\{\hat{G}^{E,f}(x_{\mathrm{B}}, x_{\mathrm{A}}, \omega)\}$, which corresponds in the time-domain to an antisymmetric signal around $t = 0$ s. Eq. (35) is one element of the 1-D version of the Green's function retrieval for coupled electromagnetic and seismic wavefields. Eq. (35) shows that the electric field response in x_B due to an elastic force source in x_A is obtained from cross-correlations of electric field recordings in x_B with particle velocity recordings recordings in x_A, both due to all four sources at the boundary as well as electric current and elastic force sources distributed throughout the domain, each source weighted with two different medium parameters. These contributions from sources throughout the domain $\mathbb{D}$ are required because wave energy is lost along the propagation paths and this must be accounted for. For practical applications we would like to ignore the contributions from sources distributed throughout the domain $\mathbb{D}$ because these sources are not likely to exist. If they would exist every source needed to be scaled according to the seismic and electric loss terms and seismoelectric coupling coefficient. The particle velocity and electric field need to be recorded simultaneously, for different source scalings, which is not naturally possible. To investigate whether it is feasible to obtain Green's functions from sources on the boundary only, we consider three simple but different configurations for numerical examples.

5 EXAMPLES

For three simple configurations we show how eq. (35) retrieves a seismoelectric Green's function. Starting from a homogeneous medium in the first example, we introduce a subsurface interface, that is, an interface between two half-spaces, in the second example. In the third

Table 1. Medium characteristics of two porous media.

Parameters	Symbol	Medium **a**	Medium **b**
Porosity	ϕ	40 per cent	20 per cent
Fluid density	ρ^f	$1.0 \times 10^3\ \mathrm{kg\,m^{-3}}$	$1.0 \times 10^3\ \mathrm{kg\,m^{-3}}$
Solid density	ρ^s	$2.7 \times 10^3\ \mathrm{kg\,m^{-3}}$	$2.7 \times 10^3\ \mathrm{kg\,m^{-3}}$
Shear Modulus of the framework	N	$9.0 \times 10^9\ \mathrm{N\,m^{-2}}$	$9.0 \times 10^9\ \mathrm{N\,m^{-2}}$
Viscosity	η	$1.0 \times 10^{-3}\ \mathrm{N\,s\,m^{-2}}$	$1.0 \times 10^{-3}\ \mathrm{N\,s\,m^{-2}}$
Rock permeability	k	$1.3 \times 10^{-12}\ \mathrm{m^2}$	$1.6 \times 10^{-12}\ \mathrm{m^2}$
Coupling Coefficient	$\mathcal{L}$	$1.0 \times 10^{-8}\ \mathrm{m^2\,s\,V^{-1}}$	$1.0 \times 10^{-9}\ \mathrm{m^2\,s\,V^{-1}}$
Tortuosity	α_∞	3.0	3.0
Permittivity of the fluid	ϵ^f	$80\epsilon_0$	$80\epsilon_0$
Permittivity of the solid	ϵ^s	$4\epsilon_0$	$4\epsilon_0$
Bulk conductivity	σ	$1.0 \times 10^{-1}\ \mathrm{S\,m^{-1}}$	$1.0 \times 10^{-1}\ \mathrm{S\,m^{-1}}$

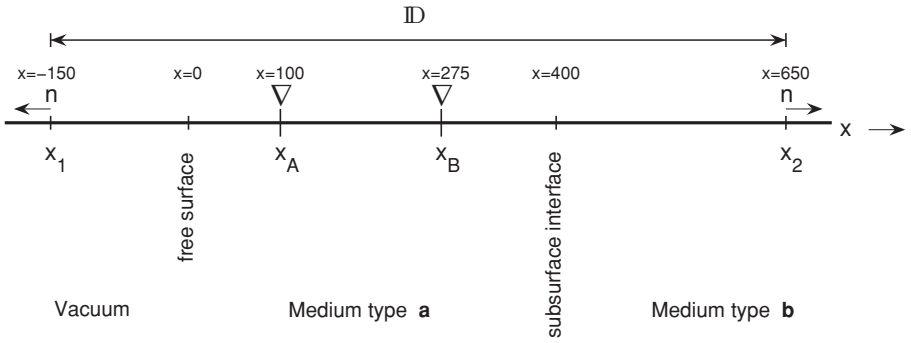

Figure 1. Geometry of the three numerical experiments. For the first experiment there are no interfaces. The second experiment introduces an interface between medium **a** and **b** below receiver B. For the third experiment there is a pressure free surface between vacuum and medium **a** above receiver A.

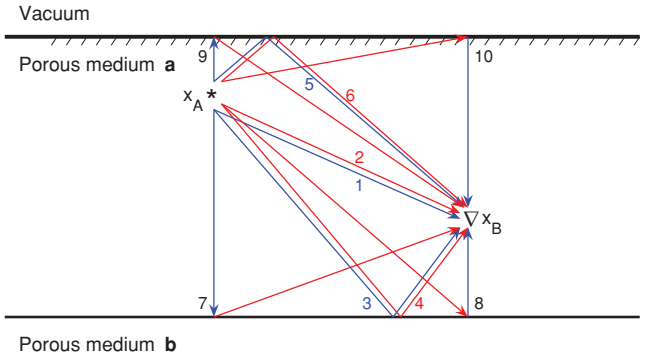

Figure 2. The ray paths of events in the seismoelectric Green's function $G^s(x_B, x_A, t)$. Red rays depict electromagnetic ray paths, blue rays depict shear wave ray paths. Events 1 and 2 are two direct events. Events 3 and 4 are reflected at the interface between medium **a** and **b**, events 7 and 8 are reflected and converted at the interface between medium **a** and **b**. Events 5 and 6 are reflected at the free surface, events 9 and 10 are reflected and converted at the free surface. In experiments 1 and 2 not all interfaces are present, and the corresponding events are not in the retrieved Green's function.

example we treat an earth-like setting with air approximated by vacuum above a two-layered earth. No seismic waves and only electromagnetic waves propagate through vacuum. We have used the Green's function solutions in a homogeneous medium, of Appendix B, to evaluate eq. (35) in the first example. In the second and third examples we have used wavefield separation techniques and a scattering formalism (Ursin 1983; Haartsen & Pride 1997; Garambois & Dietrich 2002; de Ridder 2007). We use the fixed electromagnetic parameters of free space, the velocity of light in vacuum $c_0 = 299\,792\,458\,\mathrm{m\,s^{-1}}$, $\mu_0 = 4\pi \times 10^{-7}\,\mathrm{H\,m^{-1}}$ and $\epsilon_0 = 1/(\mu_0 c_0^2)\,\mathrm{F\,m^{-1}}$ and we use two sets of variable medium parameters, sets **a** and **b** in Table 1. These media correspond to a saturated porous sandstone, with a low (Medium **a**) and high (Medium **b**) saline concentration. The configurations of all three examples are simultaneously displayed in Fig. 1. In all models we use all four source types according to eq. (35), emitting a Ricker wavelet with a central radial frequency of $\omega_c = 800\,\mathrm{radians\,s^{-1}}$.

5.1 Homogeneous space

The first example is a homogeneous space with properties of medium type **a**, see Table 1. With these parameters we have an almost frequency independent shear wave velocity of approximately $2111\,\mathrm{m\,s^{-1}}$, while the electromagnetic wavenumber has an equal real and imaginary part over almost the whole spectrum leading to a pure diffusive electromagnetic field without a well-defined propagation velocity. Receivers A and B are located at a distance of 175 m above each other. The upper boundary is located 250 m above of receiver A and the lower boundary is located 375 m below receiver B. This is indicated in Fig. 1 but now the free surface at $x = 0$ m and the interface at $x = 400$ m do not exist yet. Similarly in Fig. 2 the paths labelled 1 and 2 represent the acoustic and electromagnetic events, respectively, that occur in a homogeneous domain. The domain integral of eq. (35) is evaluated using the middle Riemann sum, with a source spacing of 0.25 m. This dense source spacing is in practise only necessary to eliminate artefacts that arise where the contribution of the domain integral should match the contribution of the boundary points. In Fig. 3, we see the time domain equivalent of the directly modelled signal, as given in the left-hand side of eq. (35), and the retrieved signal, obtained by evaluating the interferometric representation in the right-hand side of eq. (35), and they agree perfectly. The seismoelectric Green's function in homogeneous media consist of two events, see eq. (13). The first event is a purely diffusive electromagnetic field and the maximum of the diffusive time signal lies at approximately 0.58 ms. The second event travels as a shear wave and arrives after a traveltime of approximately 83 ms. The left-hand side of eq. (35) is the superposition of $G^{E,f}(x_B, x_A, t)$ and $G^{v^s,J^e}(x_A, x_B, -t)$, but we see three events in Fig. 3: the causal and time-reversed causal shear wave events, labelled 1 and the overlapping causal and time-reversed causal electromagnetic events, labelled 2, the overlap is because the arrival time of the electromagnetic event is

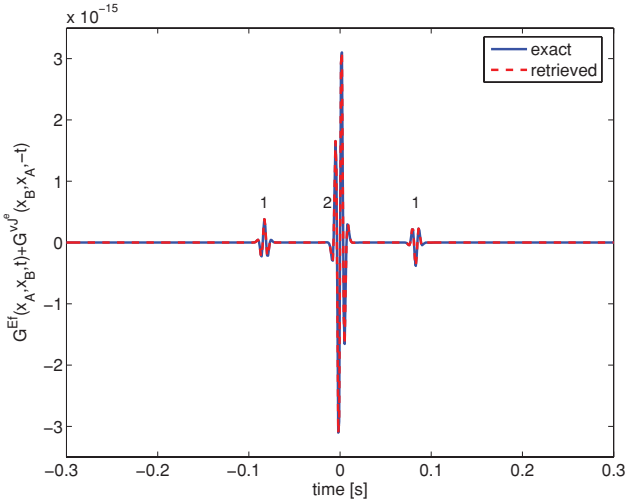

Figure 3. Exact and retrieved Green's functions, calculated by evaluating the left- and right-hand sides of eq. (35), respectively, in a homogeneous medium.

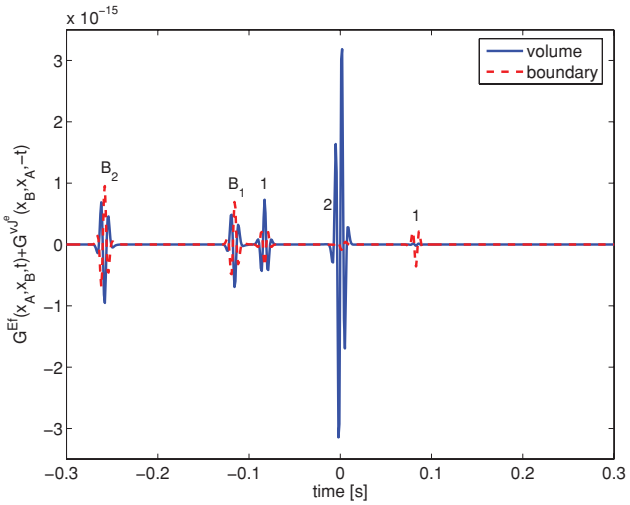

Figure 4. Separated contributions from the domain integral and the boundary points, the two terms on the right-hand side of eq. (35), to the retrieved result a homogeneous medium as shown in Fig. 3.

shorter than the side lobes of the auto-correlation of the wavelet. The fact that we retrieve a time-asymmetric Green's function convolved with a symmetric source wavelet and that there is still a retrieved response around $t = 0$, is because we subtract two equal and almost symmetric signals that are slightly displaced in time (for the time-reversed causal signal the arrival time is approximately -0.58 ms). In Fig. 4, we separated the integral contributions to the retrieved signal by sources in the domain and the two summed contributions from sources on both boundaries of the domain $\mathbb{D}$. Summing both signals results in the retrieved signal in Fig. 3. The event label numbers in Figs 3 and 4 are consistent with the ones used in Fig. 2. Note that in addition to the physical events we find two additional events in the negative time window, labelled B_1 and B_2. These correspond to cross-terms in the separate contributions of the domain integral and the boundary points, they cancel perfectly when combined. Note also how the electromagnetic event is constructed mainly by the sources in the domain integral, while the shear wave event is constructed primarily by contributions from the sources on the boundary points. This can be understood from the fact that at these seismic frequencies the electromagnetic field is primarily a diffusive field and the compensation for wave energy loss comes from the volume sources, while the loss factor of the shear wave is very small. In the positive time window, when the domain integral is neglected the amplitude error introduced in the retrieved shear wave event is less than 10 per cent. For the events in $G^{E,f}(x_\mathrm{B}, x_\mathrm{A}, t)$, this is indeed determined by the strength of the loss functions inside the domain. For the events in $G^{v^s,J^e}(x_\mathrm{A}, x_\mathrm{B}, -t)$, we see that the contribution of the boundary terms are opposite in polarity with respect to the contribution of the domain integral and the direct modelled signal. If the loss functions inside the domain are large, the boundary term contribution will be weak and the domain integral does not need to compensate that much in $G^{v^s,J^e}(x_\mathrm{A}, x_\mathrm{B}, -t)$. Fig. 5 contains a correlation gather, that is, the cross-correlation results for different positions in the domain integral of the interferometric representation. In order to cope with the large amplitude differences between the events, the colour scale depicts the logarithm of the absolute value of the signal. Summing this correlation gather results in the domain integral contribution shown in Fig. 4. Both source positions are denoted by dashed lines, the geometry of the correlation panel corresponds to the geometry as outlined in

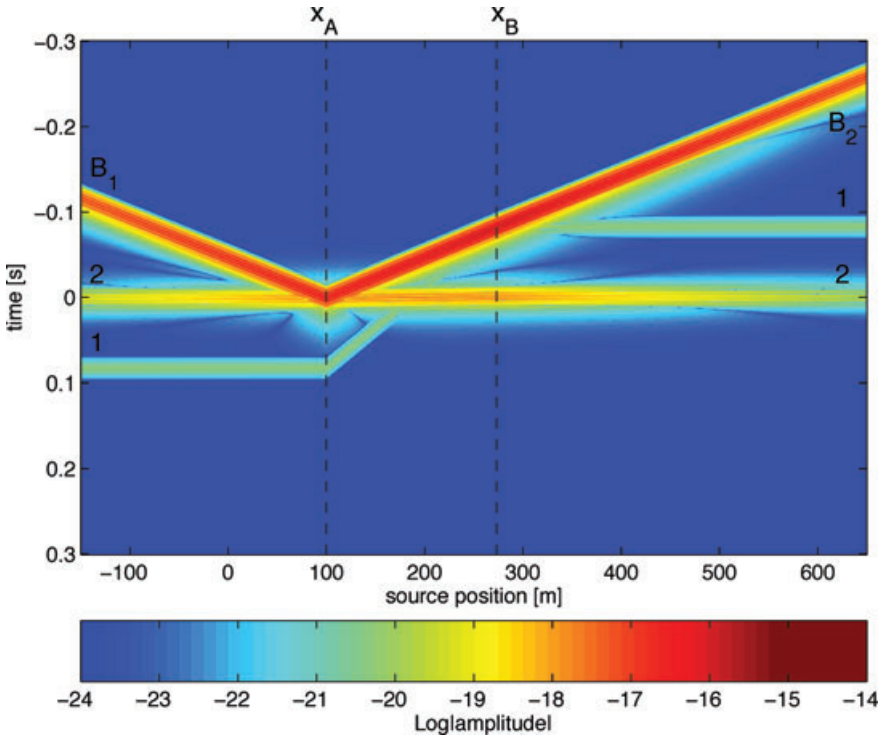

Figure 5. Correlation gather of the domain integral in a homogeneous medium, scaled as the logarithm of the absolute value. Summation of this panel would lead to the total contribution from the domain integral shown in Fig. 4. Events 1 and 2 correspond to the shear and electromagnetic direct arrivals in Fig. 2, the contributions are stationary outside the receiver span. The contributions to the spurious events B_1 and B_2 are non-stationary throughout the domain, but always reside in the negative time window.

Fig. 1. When the contribution of a certain source position to a certain event shifts in time as a function of the source position, we call those contributions non-stationary. It can be seen that for a source position located between both receivers the contributions to the physical event 1 are non-stationary. This is also the case for event 2, but since the traveltime is negligible on the seismic timescale, it is not visible. The contributions of sources in the domain integral outside the position of the receivers is stationary. This partly confirms the analysis of Snieder (2007) for seismic interferometry and Slob *et al.* (2007) for electromagnetic interferometry in dissipative media, who show that neglecting the contribution of the domain integral for weakly dissipative media will not cause spurious events, but only affect the amplitudes of the retrieved events. This is true for our physical events. For our choice of cross-correlations, the contribution to the non-physical event always resides in the negative time window. The spurious events B_1 and B_2 correspond to the correlation between a seismic and electromagnetic wave event. The correlation subtracts the long traveltime of the seismic event from a negligible traveltime of the electromagnetic event, hence the resulting traveltime of the spurious event is always negative.

5.2 Two homogeneous half-spaces

We insert an interface 125 m below receiver B, the medium below the interface has properties of medium type **b**. The seismoelectric Green's function now contains six events. The two direct waves, labelled 1 and 2 in Fig. 2, the two reflected waves, labelled 3 and 4, two waves that are converted at the reflecting interface, labelled 7 and 8. Fig. 6 shows the directly modelled signal and the accurately reconstructed retrieved signal by the interferometric representation, right-hand side of equation 35. Two small subgraphs are inserted with an exaggerated vertical scale two orders of magnitude larger, such that the arrival of the reflected shear wave, labelled 3, is visible. The electromagnetic reflected event, labelled 4, arrives after approximately 0.58 ms. The reflected shear wave, labelled 3, arrives last after a traveltime of approximately 200 ms. The converted reflected event, labelled 7, arrives after the one-way traveltime for a shear wave from receiver A to the interface of approximately 140 ms. The second converted event, labelled 8, arrives after an one-way shear wave traveltime from the interface to receiver B and it is invisible (not labelled in Fig. 6), see below. We can understand all events as coming from an elastic force source at x_A, recorded as an electrical field at x_B, as depicted in Fig. 2. Event 1 is travelling as a seismic wave directly to the receiver. Event 2 is the excited electrical field that diffuses away from the source. Event 3 is an elastic shear wave generated at the source level, reflected at the interface and propagates as a shear wave to the receiver. Event 4 is similar to event 2, but propagates to the interface first and is then reflected as an electromagnetic field back to the receiver where it is recorded. Event number 8 travels to the interface as a shear wave, where it is converted to an electromagnetic field at the interface that diffuses back to the receiver. Event 7 propagates to the interface as a shear wave, where it is converted to an electromagnetic field that diffuses back to the receiver level. Event number 8 is converted at the source to an electromagnetic

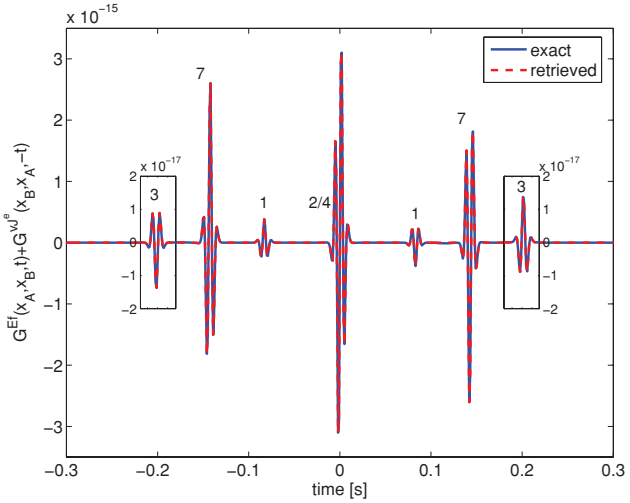

Figure 6. Exact and retrieved Green's functions, calculated by evaluating the left- and right-hand sides of eq. (35), respectively, in a two half-space medium.

field that diffuses to the interface where it is converted back to a shear wave that reflects to the receiver level, where the comoving electrical field is recorded.

To analyse the events related to the interface we can compare them to the direct events that are in this situation the same as in the first configuration of a homogeneous space. There is a negligible difference between event 2 in Fig. 3 and the combined events 2 and 4 in Fig. 6. Since the conversion for both events occurs at the receiver only, the only two reasons for a difference is the longer path between the source and receiver for event 4 leading to more attenuation of the diffuse electromagnetic field, and the electromagnetic reflection coefficient that is rather small because the electric parameters are the same for the constituents at either side of the interface apart from a porosity difference. Event 3 has a much smaller amplitude than event 1 and again the only difference is a longer propagation path and a reflection at the interface. Since the elastic wave energy loss is very small, the reason for the low amplitude is the very small reflection coefficient. In Table 1, it can be seen that the only major change across the interface is the porosity leading to a very small elastic reflection coefficient. Events 7 and 8 require a different analysis. In Fig. 2, event 8 is depicted as an event that leaves the source as an electromagnetic wave that diffuses to the interface where it is converted back into a shear wave that reflects to the receiver where the comoving electrical field is recorded. Hence, event 8 has undergone three conversions and would be too weak to measure in the field, while event 7 only experienced conversion once at the interface.

In Fig. 7, we see how the positive time window of the recovered signal, containing $G^{E,f}(x_B, x_A, t)$, is dominantly reconstructed by the contribution from sources on the boundary. In contrast, we see that the negative time window of the recovered signal, containing $G^{v^s,J^e}(x_A, x_B, -t)$, is reconstructed by approximately equally important contributions from sources in the volume and on the boundary. When the domain integral is neglected, the amplitude errors in the retrieved events 1, 3 and 7 are less than 10 per cent. The correlation gather, shown in Fig. 8, for the source positions in the domain integral is complicated by the addition of several stationary and non-stationary source positions.

Event 1 is contributing stationary to the direct shear wave event for source positions below the interface. For source positions above the interface but below receiver A it contributes stationary to the direct shear wave event and non-stationary to the shear wave reflected event 3. Source positions between receiver A and *B* contribute non-stationary to the direct shear wave and the reflected shear wave in the positive time window, but stationary to the reflected shear wave in the negative time window. For source positions above receiver B the contributions to both the direct shear wave and the reflected shear wave are stationary. It is encouraging to see that in the reconstruction of the Green's function in the positive time window the events arriving at one- or two-way seismic traveltimes are retrieved rather accurately from sources on the boundary only, while no spurious events are introduced at positive times.

5.3 Inclusion of one layer against a vacuum half-space

The last example is of a more realistic earth setting, we include a second interface 100 m above receiver A. The medium above the interface has the properties of vacuum, no shear wave, but only electromagnetic waves can propagate across the interface, but the transmission of electromagnetic energy across the interface is negligible. This interface will be referred to as the free surface. The domain integral now stretches from 0 to 650 m, we can neglect the sources on the domain boundary at the free surface, because the free surface acts as a mirror to both wave types and contributions from the vacuum medium above can be neglected (Wapenaar 2004). The Green's function contains 10 primary events, as indicated in Fig. 2, and an infinite number of multiples and free surface ghosts. Fig. 9 shows the directly modelled signal and the accurately reconstructed retrieved signal by the interferometric representation, right-hand side of eq. (35). Two inserted subgraphs with an exaggerated vertical scale two orders of magnitude larger, make event 3 visible. In addition to the events encountered in the two previous examples, we find free-surface reflected seismic and electromagnetic events, labelled 5 and 6. Two events of waves are converted at

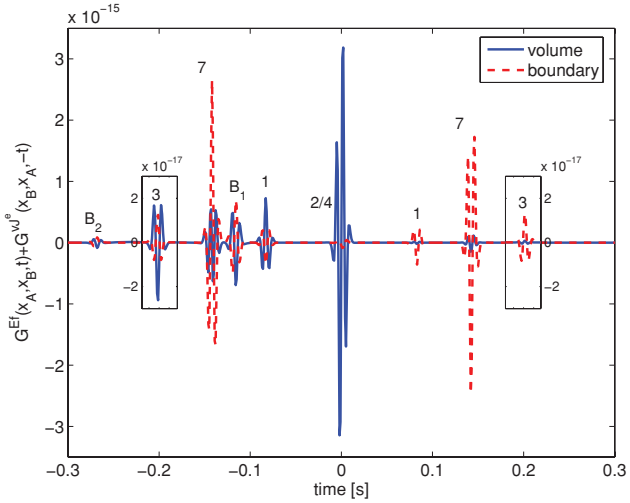

Figure 7. Separated contributions from the domain integral and the boundary points, the two terms on the right-hand side of eq. (35), to the retrieved result in a two half-space medium as shown in Fig. 6.

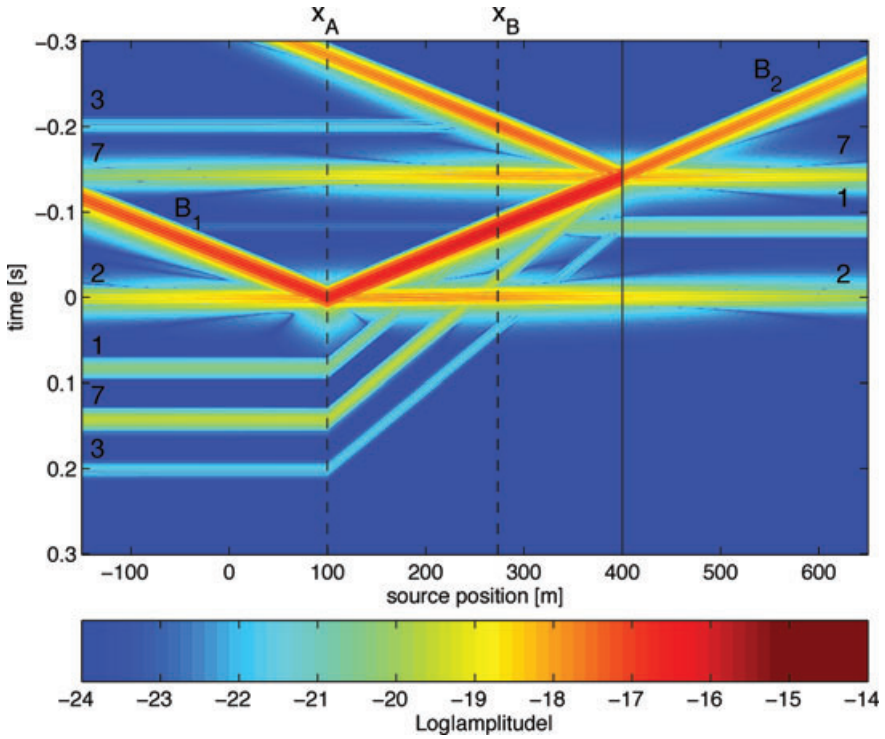

Figure 8. Correlation gather of the domain integral in a two half-space medium, scaled as the logarithm of the absolute value. Summation of this panel would lead to the total contribution from the domain integral shown in Fig. 7. In addition to the events 1, 2, B_1 and B_2, we can detect events 3 and 7 that correspond to the reflected shear wave and a converted wave as depicted in Fig. 1. All physical events have stationary contributions outside the receiver A—interface span. The contributions to the spurious events B_1 and B_2 are non-stationary throughout the domain, but always reside in the negative time window.

the interface, labelled 9 and 10, these converted reflected waves are very weak for the free surface, and cannot accurately be distinguished from the other arrivals. The free surface reflected shear wave arrives after a traveltime of approximately 180 ms. The free surface reflected electromagnetic event arrives after approximately 0.58 ms. There is one more strong event, labelled 7g, a source side shear wave free surface ghost of the subsurface converted reflected wave (labelled 7). Fig. 10 contains the separate contributions from the domain integral and the single boundary term in the interferometric representation. The positive time window of the recovered signal, containing $G^{E,f}(x_\mathrm{B}, x_\mathrm{A}, t)$, is dominantly reconstructed by just the boundary term. The negative time window of the recovered signal, containing $G^{v^s,J^e}(x_\mathrm{A}, x_\mathrm{B}, -t)$, contains strong contributions by the domain integral that correct the polarity of the contribution by the single boundary term. Just one strong non-physical event arrives within the entire time window, labelled B_2. The correlation gather, shown in Fig. 11, of the source positions in the domain integral is complicated considerably. It confirms that no strong spurious arrivals should occur in the positive time window of the retrieved signal containing $G^{E,f}(x_\mathrm{B}, x_\mathrm{A}, t)$. To illustrate how these results are of significance, we separated the contributions of the

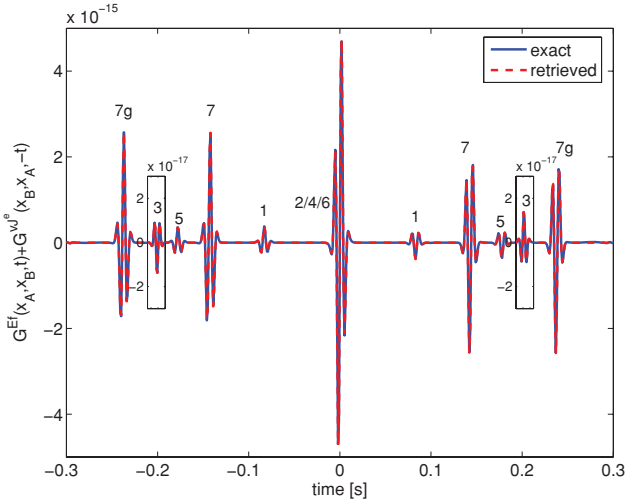

Figure 9. Exact and retrieved Green's functions, calculated by evaluating the left- and right-hand sides of eq. (35), respectively, in a two layer medium bounded by a vacuum.

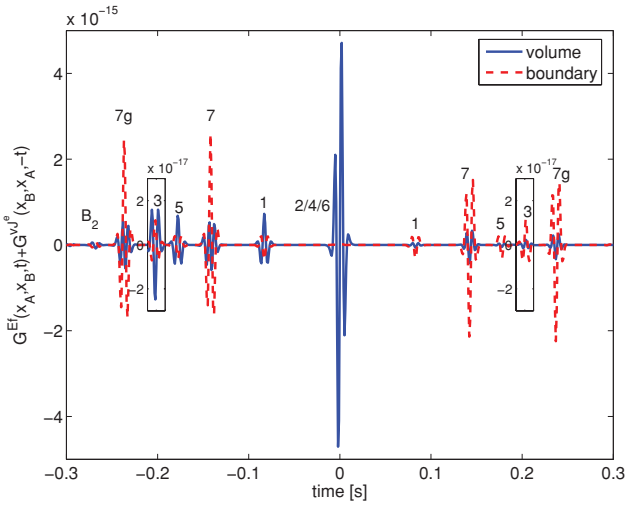

Figure 10. Separated contributions from the domain integral and the boundary points, the two terms on the right-hand side of eq. (35), to the retrieved result in a two layer medium bounded by vacuum as shown in Fig. 9.

elastodynamic source terms in the single boundary term and retrieve the positive time lags of the correlation signal in Fig. 12. Neglecting the contribution of sources inside the domain $\mathbb{D}$ results in missing the events that diffuse as electromagnetic fields and arrive approximately at $t = 0.58$ ms. This is no loss of information compared to active seismoelectric and electroseismic exploration because these responses cannot be separately recorded nor analysed. We retrieve the seismic arrivals, labelled 1, 3 and 5, which can be verified and compared with seismic experiments. The interface response and its source side ghost, which are of greatest interest, are almost completely retrieved, labelled 7 and 7g, with a amplitude error of less than 10 per cent.

6 CONCLUSIONS

We have specified known exact interferometric Green's function representations for seismic and electromagnetic wavefields to representations for the seismoelectric Green's function for coupled seismic and electromagnetic wavefields in 1-D. These representations give the seismoelectric Green's functions as function of cross-correlations of observations at two receiver stations where, respectively, the electrical field and the particle velocity are recorded. This representation consist of two terms, one representing correlations of recorded responses of sources throughout the domain of reciprocity and one representing correlations of recorded responses of sources on the boundary of the domain of reciprocity. The domain integral contains terms that cannot naturally occur or cannot be rewritten for practical application, for example observations of the same source, simultaneously operating at different strengths.

In three numerical examples we have shown how the interferometric representation retrieves the expected result. We have also investigated the effects of neglecting the sources in the domain of reciprocity, or situations in which only seismic sources exist on the boundary. In

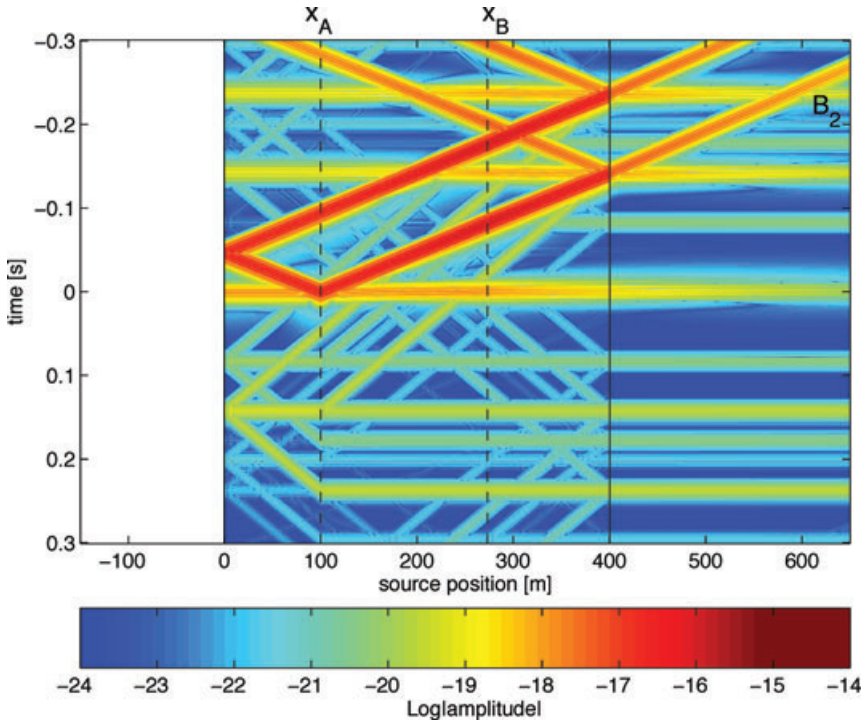

Figure 11. Correlation gather of the domain integral in a two-layer medium bounded by a vacuum, scaled as the logarithm of the absolute value. Summation of this panel would lead to the total contribution from the domain integral shown in Fig. 10. There are many more events, all physical events have stationary contributions from positions below the interface. For those positions there are still contributions to spurious events, but these always reside in the negative time window.

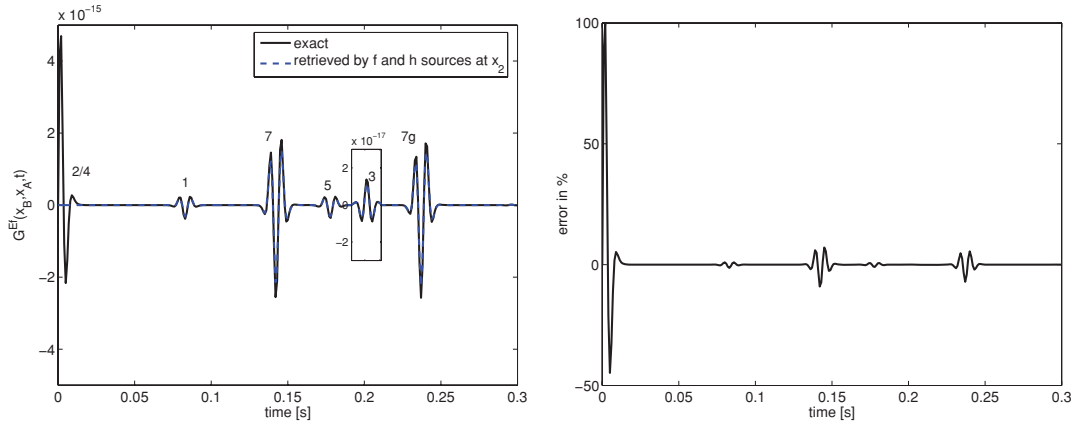

(a) (b)

Figure 12. The retrieved result for $G^{E,f}(x_B, x_A, t)$ in a two-layer medium bounded by a vacuum. In panel (a) by evaluating the interferometric integral on the right-hand side of eq. (35), neglecting the contributions from sources in the domain and the contributions from electromagnetic sources on the boundary. In panel (b), the error between the two curves in panel (a) normalized to the maximum amplitude of the exact response. The electromagnetic events 2 and 4, are almost completely absent, all other events are recovered with an error of less than 10 per cent.

homogeneous media, neglecting the sources in the domain integral leads to a spurious event on one side of the symmetrized Green's function. The amplitude error caused by neglecting the sources in the domain integral can be positive or negative. It's size depends on the wave type and travel path of the event under consideration. Since the electromagnetic field is of diffuse character, ignoring the domain sources will lead to strong amplitude errors. On the other hand, the seismic wave undergoes only weak losses, amplitude errors will therefore be weak. The spurious event that resides in one half of the retrieved symmetrized Green's function is non-stationary with respect to the location of the boundary of the domain of reciprocity, therefore the occurrence of randomly distributed noise sources on the boundary might result in destructive interference of the spurious event, similar to Draganov *et al.* (2003, 2006).

In a medium consisting of two half-spaces these conclusions are shown to hold. More precisely, all physical events have stationary contributions with respect to the boundary of the domain of reciprocity outside the domain bounded by the interface and the receiver farthest away from the interface. This means that as long as the domain of reciprocity is chosen to include both receivers and the interface, the domain

integral can be neglected. Besides amplitude errors no spurious events occur on one side of the symmetrized retrieved Green's function. Note that the first requirement, to include both receivers inside the domain of reciprocity, is a choice made to derive the interferometric Green's function representations.

In a medium consisting of two layers bounded by a vacuum, the free surface acts effectively as a mirror reflector for both wave types, thereby rendering the need for boundary sources at the surface, or electromagnetic domain sources in the vacuum, negligible. This geometry is most favourable for the use of seismoelectric interferometric Green's function representations. As long as the domain of reciprocity includes the heterogeneities, the interface between the two layers, the domain integral can be neglected and spurious events only arise on one side of the symmetrized retrieved Green's function. Amplitude errors on the events in the retrieved Green's function are as large as almost 100 per cent for the purely electromagnetic events but generally are smaller than 10 per cent for events representing wave type conversion at the interface, which are of most interest in seismoelectric exploration.

ACKNOWLEDGMENTS

The authors would like to thank Kasper van Wijk and an anonymous reviewer for helpful comments and suggestions to improve the paper. SdR would like to thank Roel Snieder for stimulating discussions on this subject when SdR was visiting Colorado School of Mines.

REFERENCES

Aki, K., 1957. Space and time spectra of stationary stochastic waves, with special reference to microtremors, *Bull. Earthq. Res. Instit.,* **35,** 415–456.

Claerbout, J.F., 1968. Synthesis of a layered medium from its acoustic transmission response, *Geophysics,* **33**(2), 264–269.

de Hoop, A.T., 1966. An elastodynamic reciprocity theorem for linear, viscoelastic media, *Appl. Sci. Res.,* **16,** 39–45.

de Hoop, A.T., 1995. *Handbook of Radiation and Scattering of Waves,* Academis Press, Amsterdam.

de Ridder, S.A.L., 2007. Simulation of Interferometric Seismoelectric Green's Function Recovery, for the SH-TE propagation mode., Master's thesis, Delft University of Technology.

Derode, A., Larose, E., Tanter, M., de Rosny, J., Tourin, A., Campillo, M. & Fink, M., 2003. Recovering the Green's function from field-field correlations in an open scattering medium (L), *J. acoust. Soc. Am.,* **113**(6), 2973–2976.

Draganov, D., Wapenaar, K. & Thorbecke, J., 2003. Synthesis of the reflection response from the transmission response in the presence of white noise sources, in *Proceedings of the 65th Annual International Meeting,* Stavanger, Norway, 2–5 June 2003, *EAGE, Extended Abstracts*, p. 218, EAGE, DB Houten, The Netherlands.

Draganov, D., Wapenaar, K. & Thorbecke, J., 2006. Seismic interferometry: Reconstructing the earth's reflection response, *Geophysics,* **71**(4), SI61–SI70.

Fokkema, J.T. & van den Berg, P.M., 1993. *Seismic Applications of Acoustic Reciprocity,* Elsevier, Amsterdam.

Garambois, S. & Dietrich, M., 2002. Full waveform numerical simulation of seismoelectromagnetic wave conversions in fluid-saturated stratified porous media, *J. geophys. Res.,* **107**(B7), 2148–2165.

Haartsen, M.W. & Pride, S.R., 1997. Electroseismic waves from point sources in layered media, *J. geophys. Res.,* **102**(B11), 24 745–24 784.

Lobkis, O. & Weaver, R., 2001. On the emergence of the green's function in the correlations of a diffuse field, *J. acoust. Soc. Am.,* **110**(6), 3011–3017.

Malcolm, A.E., Scales, J.A. & van Tiggelen, B.A., 2004. Extracting the green's function from diffuse, equipartitioned waves, *Phys. Rev. E,* **70,** 015601-1–015604-4.

Pride, S., 1994. Governing equations for the coupled electromagnetics and acoustics of porous media, *Phys. Rev. B,* **50**(21), 15 678–15 696.

Pride, S.R. & Haartsen, M.W., 1996. Electroseismic wave properties, *J. acoust. Soc. Am.,* **100**(3), 1301–1315.

Roux, P., Sabra, K.G., Kuperman, W.A. & Roux, A., 2005. Ambient noise cross correlation in free space: theoretical approach, *J. acoust. Soc. Am.,* **117**(1), 79–84.

Shapiro, N.M., Campillo, M., Stehly, L. & Ritzwoller, M.H., 2005. High-resolution surface-wave tomography from ambient seismic noise, *Science,* **307,** 1615–1618.

Slob, E., Draganov, D. & Wapenaar, K., 2006. GPR without a source, in *Proceedings of the Eleventh International Conference on Ground Penetrating Radar,* Ohio State University, Columbus, OH, p. Ant.6.

Slob, E., Draganov, D. & Wapenaar, K., 2007. Interferometric electromagnetic Green's functions representations using propagation invariants, *Geophys. J. Int.,* **169,** 60–80.

Snieder, R., 2004. Extracting the Green's function from the correlation of coda waves: a derivation based on stationary phase, *Phys. Rev. E,* **69**(4), 046610-1–046610-8.

Snieder, R., 2006. Retrieving the Green's function of the diffusion equation from the response to a random forcing, *Phys. Rev. E,* **74,** 046620-1–046620-4.

Snieder, R., 2007. Extracting the Green's function of attenuating heterogeneous acoustic media from uncorrelated waves, *J. acoust. Soc. Am.,* **121**(5), 2637–2643.

Ursin, B., 1983. Review of elastic and electromagnetic wave propagation in horizontally layered media, *Geophysics,* **48**(8), 1063–1081.

van Tiggelen, B.A., 2003. Green's function retrieval and time reversal in a disordered world, *Phys. Rev. Lett.,* **91**(24), 243 904.

Wapenaar, K., 2003. Reciprocity theorems for seismoelectric waves, *J. Seism. Expl.,* **12,** 103–112.

Wapenaar, K., 2004. Retrieving the Elastodynamic Green's function of an arbitrary inhomogeneous medium by cross correlation, *Phys. Rev. Lett.,* **93**(25), 254301-1–254301-4.

Wapenaar, K. & Fokkema, J., 2004. Reciprocity theorems for diffusion, flow, and waves, *J. Appl. Mech.,* **71,** 145–150.

Wapenaar, K., Draganov, D., Thorbecke, J. & Fokkema, J., 2002. Theory of acoustic daylight imaging revisited, in *Proceedings of the 72nd Annual Internat. Mtg. Soc. Expl. Geophys., Expanded Abstracts,* pp. 2269–2272.

Wapenaar, K., Slob, E. & Snieder, R., 2006. Unified Green's function retrieval by cross correlation, *Phys. Rev. Lett.,* **97**(23), 234301-1–234301-4.

Weaver, R.L. & Lobkis, O.I., 2001. Ultrasonics without a source: thermal fluctuation correlations at MHz frequencies, *Phys. Rev. Lett.,* **87**(13), 134301-1–134301-4.

APPENDIX A: DERIVATION OF THE SEISMOELECTRIC SYSTEM EQUATIONS IN 1-D

We start with the equations for the theory of coupled poro-elastic and electromagnetic wave propagation in dissipative inhomogeneous isotropic fluid-saturated porous media, as given by (Pride 1994). The equations of motion read

$$\partial_t \rho^b \mathbf{v}^s + \partial_t \rho^f \mathbf{w} - \partial_j \boldsymbol{\tau}_j^b = \mathbf{f}^b, \tag{A1}$$

$$\partial_t \rho^f \mathbf{v}^s + \eta k^{-1} (\mathbf{w} - \mathcal{L} * \mathbf{E}) + \nabla p^f = \mathbf{f}^f, \tag{A2}$$

with $\mathbf{w} = \phi(\mathbf{v}^s - \mathbf{v}^f)$, where $\mathbf{v}^s$ and $\mathbf{v}^f$ are the averaged particle velocities in the solid and fluid phase, respectively, $\mathbf{w}$ is the filtration velocity, ϕ is porosity, τ^b the averaged bulk stress tensor, p^f the averaged fluid pressure, and $\mathbf{E}$ the averaged electric field strength. The coupling coefficient between seismic and electromagnetic fields acts as a time-convolution operator (Pride 1994), denoted with $\mathcal{L}^*$. The source functions $\mathbf{f}^b$ and $\mathbf{f}^f$ are the volume densities of external force on the bulk and fluid, respectively. The constitutive parameters ρ^b and ρ^f are the bulk and fluid mass densities, respectively. The rock permeability k is in general a time-convolution operator (Pride 1994), but for simplicity we assume it is well represented by its static value, and η is the fluid viscosity. The linearized stress–strain relations are given by

$$-\partial_t \boldsymbol{\tau}_j^b + \mathbf{c}_{jl} \partial_l \mathbf{v}^s + \mathbf{d}_j \partial_l w_l = \mathbf{c}_{jl} \mathbf{h}_l^b + \mathbf{d}_j q^f, \tag{A3}$$

$$\partial_t p + \mathbf{d}_l^t \partial_l \mathbf{v}^s + M \partial_l w_l = \mathbf{d}_l^t \mathbf{h}_l^b + M q^f, \tag{A4}$$

where $\mathbf{d}_j$ denotes the jth column of the tensor $\mathbf{d}$. We introduced the source terms q^f and $\mathbf{h}^b$, an averaged volume injection rate and an averaged deformation rate source. For isotropic media the stiffness parameters are $d_{ij} = d\delta_{ij}$, M and $c_{ijkl} = V\delta_{ij}\delta_{kl} + N(\delta_{ik}\delta_{jl} + \delta_{il}\delta_{jk})$, where N is the shear modulus of the framework of grains, and V is dependent on N and the bulk modulus of the fluid phase, solid phase and grain framework. Maxwell's electromagnetic field equations read

$$\epsilon \partial_t \mathbf{E} + \mathbf{J} - \nabla \times \mathbf{H} = -\mathbf{J}^e, \tag{A5}$$

$$\mu \partial_t \mathbf{H} + \nabla \times \mathbf{E} = -\mathbf{J}^m, \tag{A6}$$

with $\mathbf{J}$ given by a modified Ohms Law, with coupling to the elastodynamic motion,

$$\mathbf{J} = \sigma \mathbf{E} - \mathcal{L} * \left(\nabla p^f + \frac{\partial}{\partial t} \rho^f \mathbf{v}^s - \mathbf{f}^f \right). \tag{A7}$$

The electrical constitutive parameters are ϵ, σ and μ, the electrical permittivity, electrical conductivity and magnetic permeability.

To find the equivalent system in 1-D we drop the derivatives in the first and second directions, that is, $\partial_1 = 0$ and $\partial_2 = 0$. Collecting the remaining partial differential equations for E_2, H_1, τ_{23} and υ_2^s, together with the equation for w_2, leads in the frequency domain to

$$-\mathrm{i}\omega \hat{\tau}_{23}^b + N \partial_3 \hat{\upsilon}_2^s = N \hat{h}_{23}^b + N \hat{h}_{32}^b, \tag{A8}$$

$$\mathrm{i}\omega \rho^b \hat{\upsilon}_2^s + \mathrm{i}\omega \rho^f \hat{w}_2 - \partial_3 \hat{\tau}_{23} = \hat{f}_2^b, \tag{A9}$$

$$\mathrm{i}\omega \epsilon \hat{E}_2 + \sigma \hat{E}_2 - \hat{\mathcal{L}} \left[\mathrm{i}\omega \rho^f \hat{\upsilon}_2^s - \hat{f}_2^f \right] - \partial_3 \hat{H}_1 = -\hat{J}_2^e, \tag{A10}$$

$$\mathrm{i}\omega \mu \hat{H}_1 - \partial_3 \hat{E}_2 = -\hat{J}_1^m, \tag{A11}$$

$$\mathrm{i}\omega \rho^f \hat{\upsilon}_2^s + \eta k^{-1} [\hat{w}_2 - \hat{\mathcal{L}} \hat{E}_2] = \hat{f}_2^f. \tag{A12}$$

We use eq. (A12) to eliminate w_2 from eq. (A9). It is customary to define an effective fluid density $\hat{\rho}^E = \frac{1}{\mathrm{i}\omega} \frac{\eta}{k}$, a complex bulk density $\hat{\rho}^c = (\rho^b - \frac{(\rho^f)^2}{\hat{\rho}^E})$ and an effective electric permittivity $\hat{\varepsilon} = \epsilon - i\sigma/\omega$. We simplify the source terms by defining $\hat{h}^b = \hat{h}_{23}^b + \hat{h}_{32}^b$, and include the force on the fluid phase into the external electric current source and the external force source as, $\hat{J}^e = \hat{J}_2^e + \hat{\mathcal{L}} \hat{f}_2^f$ and $\hat{f} = \hat{f}^b - \frac{\rho^f}{\hat{\rho}^E} \hat{f}^f$. Dropping all the unnecessary subscripts and denoting from here onward the x_3 coordinate by x we find

$$\mathrm{i}\omega \hat{\varepsilon} \hat{E} - \mathrm{i}\omega \rho^f \hat{\mathcal{L}} \hat{\upsilon}^s - \partial_x \hat{H} = -\hat{J}^e, \tag{A13}$$

$$\mathrm{i}\omega \mu \hat{H} - \partial_x \hat{E} = -\hat{J}^m, \tag{A14}$$

$$\mathrm{i}\omega \hat{\rho}^c \hat{\upsilon}^s + \mathrm{i}\omega \rho^f \hat{\mathcal{L}} \hat{E} - \partial_x \hat{\tau}^b = \hat{f}, \tag{A15}$$

$$-\mathrm{i}\omega N^{-1} \hat{\tau}^b + \partial_x \hat{\upsilon}^s = \hat{h}^b. \tag{A16}$$

APPENDIX B: SEISMOELECTRIC FREQUENCY DOMAIN GREEN'S FUNCTION SOLUTIONS IN 1-D HOMOGENEOUS MEDIA

We solve the 1-D seismoelectric system in homogeneous media for the fields $\hat{E}$, $\hat{H}$, $\hat{\upsilon}^s$ and $\hat{\tau}^b$. In the frequency domain, eq. (6) can be solved giving the following solution

$$\hat{\mathbf{u}} = \hat{\mathbf{G}}^m \hat{G}^s \hat{\mathbf{s}}, \tag{B1}$$

where the scalar Green's function, $\hat{G}^s$, satisfies the electroseismic wave equation,

$$\left[\partial_x^2 - \left(\mathrm{i}\omega c_{\mathrm{sh}}^{-1} \right)^2 \right] \left[\partial_x^2 - \left(\mathrm{i}\omega c_{\mathrm{te}}^{-1} \right)^2 \right] \hat{G}^s = \delta(x - x_{\mathrm{s}}), \tag{B2}$$

the wave velocities $\hat{c}_{\rm sh}$ and $\hat{c}_{\rm te}$ are the inverse of the plane wave slowness, $\hat{c}_{\rm sh,te} = 1/\hat{s}_{\rm sh,te}$ given by

$$2\hat{s}^2_{\rm sh} = \hat{\rho}^c N^{-1} + \hat{\varepsilon}\mu + \sqrt{(\hat{\rho}^c N^{-1} - \hat{\varepsilon}\mu)^2 - 4\mu N^{-1}(\rho^f \hat{\mathcal{L}})^2}, \tag{B3}$$

$$2\hat{s}^2_{\rm te} = \hat{\rho}^c N^{-1} + \hat{\varepsilon}\mu - \sqrt{(\hat{\rho}^c N^{-1} - \hat{\varepsilon}\mu)^2 - 4\mu N^{-1}(\rho^f \hat{\mathcal{L}})^2}. \tag{B4}$$

The matrix $\hat{\mathbf{G}}^m$ in the right-hand side of eq. (B1) is an operator matrix linking the sources terms to the fields, this is the non-scalar part of the seismoelectric Green's function solutions. The matrix Green's function is obtained as $\hat{\mathbf{G}}(x, x_{\rm s}, \omega) = \hat{\mathbf{G}}^m \hat{G}^s(x, x_{\rm s}, \omega)$ and the elements of the Green's matrix $\hat{\mathbf{G}}$ are given by

$$\hat{G}^{E,J^e}(x, x_{\rm s}, \omega) = \left[\{{\rm i}\omega\}^3 \mu \frac{\hat{\rho}^c}{N} - {\rm i}\omega\mu\partial_x^2\right] \hat{G}^s(x, x_{\rm s}, \omega), \tag{B5}$$

$$\hat{G}^{E,J^m}(x, x_{\rm s}, \omega) = \left[\{{\rm i}\omega\}^2 \frac{\hat{\rho}^c}{N}\partial_x - \partial_x^3\right] \hat{G}^s(x, x_{\rm s}, \omega), \tag{B6}$$

$$\hat{G}^{E,f}(x, x_{\rm s}, \omega) = \left[\{{\rm i}\omega\}^3 \frac{\rho^f \hat{\mathcal{L}}}{N}\mu\right] \hat{G}^s(x, x_{\rm s}, \omega), \tag{B7}$$

$$\hat{G}^{E,h^b}(x, x_{\rm s}, \omega) = -\left[\{{\rm i}\omega\}^2 \rho^f \hat{\mathcal{L}}\mu\partial_x\right] \hat{G}^s(x, x_{\rm s}, \omega), \tag{B8}$$

$$\hat{G}^{H,J^e}(x, x_{\rm s}, \omega) = \left[\{{\rm i}\omega\}^2 \frac{\hat{\rho}^c}{N}\partial_x - \partial_x^3\right] \hat{G}^s(x, x_{\rm s}, \omega), \tag{B9}$$

$$\hat{G}^{H,J^m}(x, x_{\rm s}, \omega) = -\left\{{\rm i}\omega\varepsilon\partial_x^2 - \{{\rm i}\omega\}^3 \left[\frac{\hat{\rho}^c}{N}\hat{\varepsilon} + \frac{\left(\rho^f \hat{\mathcal{L}}\right)^2}{N}\right]\right\} \hat{G}^s(x, x_{\rm s}, \omega), \tag{B10}$$

$$\hat{G}^{H,f}(x, x_{\rm s}, \omega) = \left[\{{\rm i}\omega\}^2 \frac{\rho^f \hat{\mathcal{L}}}{N}\partial_x\right] \hat{G}^s(x, x_{\rm s}, \omega), \tag{B11}$$

$$\hat{G}^{H,h^b}(x, x_{\rm s}, \omega) = -\left[{\rm i}\omega\rho^f \hat{\mathcal{L}}\partial_x^2\right] \hat{G}^s(x, x_{\rm s}, \omega), \tag{B12}$$

$$\hat{G}^{v^s,J^e}(x, x_{\rm s}, \omega) = -\left[\{{\rm i}\omega\}^3 \frac{\rho^f \mu \hat{\mathcal{L}}}{N}\mu\right] \hat{G}^s(x, x_{\rm s}, \omega), \tag{B13}$$

$$\hat{G}^{v^s,J^m}(x, x_{\rm s}, \omega) = -\left[\{{\rm i}\omega\}^2 \frac{\rho^f \hat{\mathcal{L}}}{N}\partial_x\right] \hat{G}^s(x, x_{\rm s}, \omega), \tag{B14}$$

$$\hat{G}^{v^s,f}(x, x_{\rm s}, \omega) = \left[\{{\rm i}\omega\}^3 \frac{\hat{\varepsilon}\mu}{N} - {\rm i}\omega\frac{1}{N}\partial_x^2\right] \hat{G}^s(x, x_{\rm s}, \omega), \tag{B15}$$

$$\hat{G}^{v^s,h^b}(x, x_{\rm s}, \omega) = \left[\partial_x^3 - \{{\rm i}\omega\}^2 \hat{\varepsilon}\mu\partial_x\right] \hat{G}^s(x, x_{\rm s}, \omega), \tag{B16}$$

$$\hat{G}^{\tau^b,J^e}(x, x_{\rm s}, \omega) = \left[\{{\rm i}\omega\}^2 \rho^f \hat{\mathcal{L}}\mu\partial_x\right] \hat{G}^s(x, x_{\rm s}, \omega), \tag{B17}$$

$$\hat{G}^{\tau^b,J^m}(x, x_{\rm s}, \omega) = \left[{\rm i}\omega\rho^f \hat{\mathcal{L}}\partial_x^2\right] \hat{G}^s(x, x_{\rm s}, \omega), \tag{B18}$$

$$\hat{G}^{\tau^b,f}(x, x_{\rm s}, \omega) = \left[\partial_x^3 - \{{\rm i}\omega\}^2 \hat{\varepsilon}\mu\partial_x\right] \hat{G}^s(x, x_{\rm s}, \omega), \tag{B19}$$

$$\hat{G}^{\tau^b,h^b}(x, x_{\rm s}, \omega) = -\left\{{\rm i}\omega\hat{\rho}^c\partial_x^2 - \{{\rm i}\omega\}^3 \left[\hat{\varepsilon}\mu\hat{\rho}^c + (\rho^f \hat{\mathcal{L}})^2\mu\right]\right\} \hat{G}^s(x, x_{\rm s}, \omega). \tag{B20}$$

Now we solve eq. (B2) for the scalar Green's function. Defining a spatial Fourier transformation as

$$\tilde{G}(k, \omega) = \int_{-\infty}^{\infty} \hat{G}(x, \omega) \exp({\rm i}kx){\rm d}x, \tag{B21}$$

eq. (B2) can be solved in the wavenumber–frequency domain,

$$\tilde{G}^s(k, \omega) = \left[\{{\rm i}k\}^2 - \{{\rm i}\omega\hat{s}_{\rm sh}\}^2\right]^{-1} \left[\{{\rm i}k\}^2 - \{{\rm i}\omega\hat{s}_{\rm te}\}^2\right]^{-1}. \tag{B22}$$

Eq. (B22) can be written as

$$\tilde{G}^s(k, \omega) = -\left[\{{\rm i}\omega\hat{s}_{\rm sh}\}^2 - \{{\rm i}\omega\hat{s}_{\rm te}\}^2\right]^{-1} \left[\left(\{{\rm i}k\}^2 - \{{\rm i}\omega\hat{s}_{\rm te}\}^2\right)^{-1} - \left(\{{\rm i}k\}^2 - \{{\rm i}\omega\hat{s}_{\rm sh}\}^2\right)^{-1}\right]. \tag{B23}$$

This implies that the scalar Green's function is the weighted sum of two Green's functions, each satisfying a modified Helmholtz equation

$$\left[\partial_x \partial_x - \{\mathrm{i}\omega \hat{s}_{\mathrm{sh}}\}^2\right] \hat{G}^s_{\mathrm{sh;te}}(x, x_{\mathrm{s}}, \omega) = -\delta(x - x_s). \tag{B24}$$

The solution to this equation is well known,

$$\hat{G}^s_{\mathrm{sh;te}}(x, x_{\mathrm{s}}, \omega) = \frac{\exp\left(-\mathrm{i}\omega \hat{s}_{\mathrm{sh;te}}\,|x - x_s|\right)}{2\mathrm{i}\omega \hat{s}_{\mathrm{sh;te}}}, \tag{B25}$$

and the complete scalar Green's function is given by,

$$\hat{G}^s(x, x_{\mathrm{s}}, \omega) = \frac{\hat{G}^s_{\mathrm{te}}(x, x_{\mathrm{s}}, \omega) - \hat{G}^s_{\mathrm{sh}}(x, x_{\mathrm{s}}, \omega)}{\{\mathrm{i}\omega \hat{s}_{\mathrm{sh}}\}^2 - \{\mathrm{i}\omega \hat{s}_{\mathrm{te}}\}^2}. \tag{B26}$$

The first two derivatives of the partial Green's functions are given by

$$\partial_x \hat{G}^s_{\mathrm{sh;te}}(x, x_{\mathrm{s}}, \omega) = -\frac{1}{2}\mathrm{sign}(x - x_s) \exp\left(-\mathrm{i}\omega \hat{s}_{\mathrm{sh;te}}\,|x - x_s|\right), \tag{B27}$$

$$\partial_x \partial_x \hat{G}^s_{\mathrm{sh;te}}(x, x_{\mathrm{s}}, \omega) = -\delta(x - x_s) + \left\{\mathrm{i}\omega \hat{s}_{\mathrm{sh;te}}\right\}^2 \hat{G}^s_{\mathrm{sh;te}}(x, x_{\mathrm{s}}, \omega), \tag{B28}$$

and hence the first three derivatives acting on the full scalar Green's function are given by

$$\partial_x \hat{G}^s(x, x_{\mathrm{s}}, \omega) = -\mathrm{sign}(x - x_s) \frac{\{\mathrm{i}\omega \hat{s}_{\mathrm{te}}\}\, \hat{G}^s_{\mathrm{te}}(x, x_{\mathrm{s}}, \omega) - \{\mathrm{i}\omega \hat{s}_{\mathrm{sh}}\}\, \hat{G}^s_{\mathrm{sh}}(x, x_{\mathrm{s}}, \omega)}{\{\mathrm{i}\omega \hat{s}_{\mathrm{sh}}\}^2 - \{\mathrm{i}\omega \hat{s}_{\mathrm{te}}\}^2}, \tag{B29}$$

$$\partial_x \partial_x \hat{G}^s(x, x_{\mathrm{s}}, \omega) = \frac{\{\mathrm{i}\omega \hat{s}_{\mathrm{te}}\}^2\, \hat{G}^s_{\mathrm{te}}(x, x_{\mathrm{s}}, \omega) - \{\mathrm{i}\omega \hat{s}_{\mathrm{sh}}\}^2\, \hat{G}^s_{\mathrm{sh}}(x, x_{\mathrm{s}}, \omega)}{\{\mathrm{i}\omega \hat{s}_{\mathrm{sh}}\}^2 - \{\mathrm{i}\omega \hat{s}_{\mathrm{te}}\}^2}, \tag{B30}$$

$$\partial_x \partial_x \partial_x \hat{G}^s(x, x_{\mathrm{s}}, \omega) = -\mathrm{sign}(x - x_s) \frac{\{\mathrm{i}\omega \hat{s}_{\mathrm{te}}\}^3\, \hat{G}^s_{\mathrm{te}}(x, x_{\mathrm{s}}, \omega) - \{\mathrm{i}\omega \hat{s}_{\mathrm{sh}}\}^3\, \hat{G}^s_{\mathrm{sh}}(x, x_{\mathrm{s}}, \omega)}{\{\mathrm{i}\omega \hat{s}_{\mathrm{sh}}\}^2 - \{\mathrm{i}\omega \hat{s}_{\mathrm{te}}\}^2}. \tag{B31}$$

This completes the solution.

Errata, see equations 16 and 34

$\hat{\mathbf{u}} \rightarrow \hat{\mathbf{G}}(x, x_s, \omega)$. The Green's matrix obeys the matrix eq. (6),

$$\mathrm{i}\omega\hat{\mathbf{A}}\hat{\mathbf{G}}(x, x_s, \omega) + \mathbf{D}_x\hat{\mathbf{G}}(x, x_s, \omega) = \mathbf{I}\delta(x - x_s). \tag{11}$$

All elements of the Green's matrix have dimension (m^{-1}) and are distinguished by their superscript containing the field type and source type, the Green's matrix for the 1-D seismoelectric system is given by

$$\hat{\mathbf{G}}(x, x_s, \omega) = \begin{bmatrix} \hat{G}^{E,J^e}(x, x_s, \omega) & \hat{G}^{E,J^m}(x, x_s, \omega) & \hat{G}^{E,f}(x, x_s, \omega) & \hat{G}^{E,h^b}(x, x_s, \omega) \\ \hat{G}^{H,J^e}(x, x_s, \omega) & \hat{G}^{H,J^m}(x, x_s, \omega) & \hat{G}^{H,f}(x, x_s, \omega) & \hat{G}^{H,h^b}(x, x_s, \omega) \\ \hat{G}^{v^s,J^e}(x, x_s, \omega) & \hat{G}^{v^s,J^m}(x, x_s, \omega) & \hat{G}^{v^s,f}(x, x_s, \omega) & \hat{G}^{v^s,h^b}(x, x_s, \omega) \\ \hat{G}^{\tau^b,J^e}(x, x_s, \omega) & \hat{G}^{\tau^b,J^m}(x, x_s, \omega) & \hat{G}^{\tau^b,f}(x, x_s, \omega). & \hat{G}^{\tau^b,h^b}(x, x_s, \omega) \end{bmatrix}. \tag{12}$$

The notation $\hat{G}^{v^s,J^e}(x, x_s, \omega)$ denotes a particle velocity response measured at x due to an impulsive electrical current source acting at $x = x_s$, in the frequency domain. In Appendix B, we derive Green's function solutions for a homogeneous medium. The scalar part of the Green's matrix can be seen to contain two events travelling with different velocities,

$$\hat{G}^s(x, x_s, \omega) = \frac{\hat{G}^s_{\mathrm{te}}(x, x_s, \omega) - \hat{G}^s_{\mathrm{sh}}(x, x_s, \omega)}{\{\mathrm{i}\omega\hat{s}_{\mathrm{sh}}\}^2 - \{\mathrm{i}\omega\hat{s}_{\mathrm{te}}\}^2}, \tag{13}$$

where $\hat{s}_{\mathrm{sh}}$ and $\hat{s}_{\mathrm{te}}$ are the seismic and electromagnetic slownesses, respectively. Because $\hat{s}_{\mathrm{sh}} \gg \hat{s}_{\mathrm{te}}$, the seismic slowness dominates the scaling of the scalar part of the seismoelectric Green's function in homogeneous media. The partial Green's functions $\hat{G}^s_{\mathrm{sh}}(x, x_s, \omega)$ and $\hat{G}^s_{\mathrm{te}}(x, x_s, \omega)$ are each, respectively, given by

$$\hat{G}^s_{\mathrm{sh;te}}(x, x_s, \omega) = \frac{\exp\left(-\mathrm{i}\omega\hat{s}_{\mathrm{sh;te}}\,|x - x_s|\right)}{2\mathrm{i}\omega\hat{s}_{\mathrm{sh;te}}}. \tag{14}$$

This means that seismoelectric conversion takes place at the source and at the receiver. This can be understood from eqs (2) to (5). An electrical current source excites both the electric and magnetic fields as well as the particle velocity through the coupling coefficient. In heterogeneous media conversion of wave types will also occur at interfaces where the material properties change (Haartsen & Pride 1997).

3 CONVOLUTION TYPE RECIPROCITY THEOREM

A reciprocity theorem interrelates two independent states in one and the same domain (de Hoop 1966; Fokkema & van den Berg 1993). The basis for reciprocity theorems is the application of the theorem of Gauss over an interaction quantity that interrelates the two states. We consider two physical states, distinguished with subscripts A and B, in a 1-D domain $\mathbb{D}$, with boundary points $x = x_1$ and $x = x_2$ and outward pointing normals n_1 and n_2. We choose $x_1 < x_2$ and find outward pointing normal vectors $n_1 = -1$ and $n_2 = 1$. The material parameters and the source functions may be different in both states. We consider the interaction quantity

$$\partial_x\left(\hat{E}_A\hat{H}_B - \hat{H}_A\hat{E}_B + \hat{\tau}^b_A\hat{v}^s_B - \hat{v}^s_A\hat{\tau}^b_B\right). \tag{15}$$

This interaction quantity is the summation of the convolution type interaction quantities commonly used in the uncoupled electromagnetic and elastodynamic systems (de Hoop 1995; Wapenaar 2003). Substitution of eqs (2)–(5) for the fields in states A and B into eq. (15), integrating over the domain $\mathbb{D}$ from x_1 to x_2 and applying the theorem of Gauss, leads to the convolution type reciprocity theorem

$$\begin{aligned} &\left\{\hat{E}_A\hat{H}_B - \hat{H}_A\hat{E}_B + \hat{\tau}^b_A\hat{v}^s_B - \hat{v}^s_A\hat{\tau}^b_B\right\}\Big|_{x_1}^{x_2} \\ &= \int_{\mathbb{D}}\left\{\hat{E}_A\hat{J}^e_B - \hat{E}_B\hat{J}^e_A + \hat{H}_A\hat{J}^m_B - \hat{H}_B\hat{J}^m_A + \hat{v}^s_A\hat{f}_B - \hat{v}^s_B\hat{f}_A + \hat{\tau}^b_A\hat{h}^b_B - \hat{\tau}^b_B\hat{h}^b_A\right\}\mathrm{d}x \\ &\quad + \mathrm{i}\omega\int_{\mathbb{D}}\left\{-\hat{E}_A\left(\hat{\varepsilon}_A - \hat{\varepsilon}_B\right)\hat{E}_B + \hat{E}_A\left(\rho^f_A\hat{\mathcal{L}}_A - \rho^f_B\hat{\mathcal{L}}_B\right)\hat{v}^s_B + \hat{v}^s_A\left(\rho^f_A\hat{\mathcal{L}}_A - \rho^f_B\hat{\mathcal{L}}_B\right)\hat{E}_B\right. \\ &\quad \left. + \hat{v}^s_A\left(\hat{\rho}^c_A - \hat{\rho}^c_B\right)\hat{v}^s_B + \hat{H}_A\left(\mu_A - \mu_B\right)\hat{H}_B - \hat{\tau}^b_A\left(N_A^{-1} - N_B^{-1}\right)\hat{\tau}^b_B\right\}\mathrm{d}x. \end{aligned} \tag{16}$$

This is the 1-D equivalent of the convolution type reciprocity integral for the full 3-D seismoelectric system of Pride, previously derived by Wapenaar (2003). We speak of a convolution type reciprocity theorem, because the multiplications in the frequency domain correspond to convolutions in the time domain. A similar equation for the general matrix eq. (6) was derived by Wapenaar & Fokkema (2004),

$$\left\{\hat{\mathbf{u}}^T_A\mathbf{K}\mathbf{N}_x\hat{\mathbf{u}}_B\right\}\Big|_{x_1}^{x_2} = \int_{\mathbb{D}}\left\{\hat{\mathbf{u}}^T_A\mathbf{K}\hat{\mathbf{s}}_B - \hat{\mathbf{s}}^T_A\mathbf{K}\hat{\mathbf{u}}_B\right\}\mathrm{d}x + \mathrm{i}\omega\int_{\mathbb{D}}\left\{\hat{\mathbf{u}}^T_A\mathbf{K}\left[\hat{\mathbf{A}}_A - \hat{\mathbf{A}}_B\right]\hat{\mathbf{u}}_B\right\}\mathrm{d}x, \tag{17}$$

where $\mathbf{N}_x$ is a matrix containing normal vectors arising after the application of the theorem of Gauss, it has the same structure as the matrix $\mathbf{D}_x$ but with all partial derivatives replaced by the unit value,

$$\mathbf{N}_x = \begin{pmatrix} 0 & -1 & 0 & 0 \\ -1 & 0 & 0 & 0 \\ 0 & 0 & 0 & 1 \\ 0 & 0 & 1 & 0 \end{pmatrix}. \tag{18}$$

$\hat{\mathbf{G}}(x, x_A, \omega)$ and $\hat{\mathbf{G}}(x, x_B, \omega)$ into eq. (32), and using the symmetry property of the Green's matrix of eq. (20) we find

$$\begin{aligned}&\hat{\mathbf{G}}(x_A, x_B, \omega) + \hat{\mathbf{G}}^{\dagger}(x_B, x_A, \omega)\\ &\quad= \left\{\hat{\mathbf{G}}^{\dagger}(x, x_A, \omega)\mathbf{N}_{\mathrm{x}}\hat{\mathbf{G}}(x, x_B, \omega)\right\}\Big|_{x_1}^{x_2} + \int_{\mathbb{D}}\left\{\hat{\mathbf{G}}^{\dagger}(x, x_A, \omega)\left[\mathrm{i}\omega\left(\hat{\mathbf{A}}_B - \hat{\mathbf{A}}_A^{\dagger}\right)\right]\hat{\mathbf{G}}(x, x_B, \omega)\right\}\mathrm{d}x.\end{aligned} \tag{33}$$

4.1 Interferometric Green's function representation

A third integral representation is a novel interpretation of the correlation type reciprocity theorem. Applying the source receiver reciprocity relation for the Green's matrix into the correlation type reciprocity theorem for the Green's matrix, eq. (33), using the symmetry properties of the matrices $\mathbf{D}_{\mathrm{x}}$ and $\hat{\mathbf{A}}$ and transposing the entire equation, we find

$$\begin{aligned}&\hat{\mathbf{G}}(x_B, x_A, \omega) + \hat{\mathbf{G}}^{\dagger}(x_A, x_B, \omega)\\ &\quad= \left\{\hat{\mathbf{G}}(x_B, x, \omega)\mathbf{N}_{\mathrm{x}}\hat{\mathbf{G}}^{\dagger}(x_A, x, \omega)\right\}\Big|_{x_1}^{x_2} + \int_{\mathbb{D}}\left\{\hat{\mathbf{G}}(x_B, x, \omega)\left[\mathrm{i}\omega\left(\hat{\mathbf{A}}_B - \hat{\mathbf{A}}_A^{\dagger}\right)\right]\hat{\mathbf{G}}^{\dagger}(x_A, x, \omega)\right\}\mathrm{d}x,\end{aligned} \tag{34}$$

which is the interferometric Green's function representation as derived by Wapenaar *et al.* (2006). We expand the $\{1, 3\}$ element of the left-hand side of eq. (34), using the Green's matrix of eq. (12) and the normal vectors in $\mathbf{N}_{\mathrm{x}}$ of eq. (18), assuming that states A and B have equal medium parameters, and the sources emit a signal with a power spectrum $\hat{S}$,

$$\begin{aligned}&\left\{\hat{G}^{E,f}(x_{\mathrm{B}}, x_{\mathrm{A}}, \omega) + \hat{G}^{v^s,J^e*}(x_{\mathrm{A}}, x_{\mathrm{B}}, \omega)\right\}\hat{S}\\ &\quad= \Big\{\hat{G}^{E,J^e}(x_{\mathrm{B}}, x, \omega)\hat{G}^{v,J^m*}(x_{\mathrm{A}}, x, \omega) + \hat{G}^{E,J^m}(x_{\mathrm{B}}, x, \omega)\hat{G}^{v,J^e*}(x_{\mathrm{A}}, x, \omega)\\ &\qquad- \hat{G}^{E,f}(x_{\mathrm{B}}, x, \omega)\hat{G}^{v,h*}(x_{\mathrm{A}}, x, \omega) - \hat{G}^{E,h}(x_{\mathrm{B}}, x, \omega)\hat{G}^{v,f*}(x_{\mathrm{A}}, x, \omega)\Big\}\Big|_{x_1}^{x_2}\ \hat{S}\\ &\qquad+ \mathrm{i}\omega 2\int_{\mathbb{D}}\Big\{\hat{G}^{E,J^e}(x_{\mathrm{B}}, x, \omega)\mathrm{i}\Im\{\hat{\varepsilon}\}\hat{G}^{v,J^e*}(x_{\mathrm{A}}, x, \omega) + \hat{G}^{E,f}(x_{\mathrm{B}}, x, \omega)\Re\{\rho^f\hat{\mathcal{L}}\}\hat{G}^{v,J^e*}(x_{\mathrm{A}}, x, \omega)\\ &\qquad- \hat{G}^{E,J^e}(x_{\mathrm{B}}, x, \omega)\Re\{\rho^f\hat{\mathcal{L}}\}\hat{G}^{v,f*}(x_{\mathrm{A}}, x, \omega) + \hat{G}^{E,f}(x_{\mathrm{B}}, x, \omega)i\Im\{\hat{\rho}^c\}\hat{G}^{v,f*}(x_{\mathrm{A}}, x, \omega)\Big\}\mathrm{d}x\ \hat{S}.\end{aligned} \tag{35}$$

According to source–receiver reciprocity expressed in eq. (22), we have $\hat{G}^{v^s,J^e}(x_{\mathrm{A}}, x_{\mathrm{B}}, \omega) = -\hat{G}^{E,f}(x_{\mathrm{B}}, x_{\mathrm{A}}, \omega)$. Thus on the left-hand side side of eq. (35) we retrieve $i\,2\,\Im\{\hat{G}^{E,f}(x_{\mathrm{B}}, x_{\mathrm{A}}, \omega)\}$, which corresponds in the time-domain to an antisymmetric signal around $t = 0$ s. Eq. (35) is one element of the 1-D version of the Green's function retrieval for coupled electromagnetic and seismic wavefields. Eq. (35) shows that the electric field response in x_B due to an elastic force source in x_A is obtained from cross-correlations of electric field recordings in x_B with particle velocity recordings recordings in x_A, both due to all four sources at the boundary as well as electric current and elastic force sources distributed throughout the domain, each source weighted with two different medium parameters. These contributions from sources throughout the domain $\mathbb{D}$ are required because wave energy is lost along the propagation paths and this must be accounted for. For practical applications we would like to ignore the contributions from sources distributed throughout the domain $\mathbb{D}$ because these sources are not likely to exist. If they would exist every source needed to be scaled according to the seismic and electric loss terms and seismoelectric coupling coefficient. The particle velocity and electric field need to be recorded simultaneously, for different source scalings, which is not naturally possible. To investigate whether it is feasible to obtain Green's functions from sources on the boundary only, we consider three simple but different configurations for numerical examples.

5 EXAMPLES

For three simple configurations we show how eq. (35) retrieves a seismoelectric Green's function. Starting from a homogeneous medium in the first example, we introduce a subsurface interface, that is, an interface between two half-spaces, in the second example. In the third

Table 1. Medium characteristics of two porous media.

Parameters	Symbol	Medium **a**	Medium **b**
Porosity	ϕ	40 per cent	20 per cent
Fluid density	ρ^f	$1.0 \times 10^3\ \mathrm{kg\,m^{-3}}$	$1.0 \times 10^3\ \mathrm{kg\,m^{-3}}$
Solid density	ρ^s	$2.7 \times 10^3\ \mathrm{kg\,m^{-3}}$	$2.7 \times 10^3\ \mathrm{kg\,m^{-3}}$
Shear Modulus of the framework	N	$9.0 \times 10^9\ \mathrm{N\,m^{-2}}$	$9.0 \times 10^9\ \mathrm{N\,m^{-2}}$
Viscosity	η	$1.0 \times 10^{-3}\ \mathrm{N\,s\,m^{-2}}$	$1.0 \times 10^{-3}\ \mathrm{N\,s\,m^{-2}}$
Rock permeability	k	$1.3 \times 10^{-12}\ \mathrm{m^2}$	$1.6 \times 10^{-12}\ \mathrm{m^2}$
Coupling Coefficient	$\mathcal{L}$	$1.0 \times 10^{-8}\ \mathrm{m^2\,s\,V^{-1}}$	$1.0 \times 10^{-9}\ \mathrm{m^2\,s\,V^{-1}}$
Tortuosity	α_∞	3.0	3.0
Permittivity of the fluid	ϵ^f	$80\epsilon_0$	$80\epsilon_0$
Permittivity of the solid	ϵ^s	$4\epsilon_0$	$4\epsilon_0$
Bulk conductivity	σ	$1.0 \times 10^{-1}\ \mathrm{S\,m^{-1}}$	$1.0 \times 10^{-1}\ \mathrm{S\,m^{-1}}$